The effect of spatial organization of peatland patterns on the hydrology

Marloes Arens

Final version
July 2017

MSc thesis
Soil Geography and Landscape Group
Wageningen University
Supervisors: JJ Nijp, dr.ir. AJAM Temme, drs. PJJF Torfs, dr.ir. AJ Teuling

Abstract

Climate change is predicted to cause more intense and less frequent precipitation events in Scandinavia. This will cause longer droughts with larger water deficits, which will result in lower groundwater tables. When a lowering of the water table occurs in peatlands, the peat will start to decompose. This turns the peatlands from a carbon sink into a carbon source, which further enhances climate change. Current models used to calculate the lowering of the water table do not take into account the spatial patterns of hummocks and hollows present in peatland, though a difference in hydraulic conductivity between these pattern entities is found, which might make peatlands more resilient than now assumed. This study focusses on the effect that spatial organization of hummock-hollow patterns have on the hydrology of peatlands. Field work on the variation in hydraulic conductivity was performed at Degerö Stormyr, a mire in Sweden. With 87 hydraulic conductivity measurements distributed between 10 and 150 cm depth in hummocks and hollows, a significant difference was found; hollows have a significantly higher hydraulic conductivity until a depth of 90 cm, after which no significant difference is found.

This data was used to create a model on a small domain (100 by 70 m) where various hummock-hollow pattern scenarios were implemented. The model was used to simulate the response of peat water holding capacity to an extreme precipitation event followed by a dry period. In total 9 pattern scenarios were used to test the effect of distance between hummocks, the orientation of the pattern, and the spatial organization of hummocks and hollows. It was found that a greater distance between hummocks results in longer water retention within the model domain. A pattern orientation parallel to the stream direction showed to dry out slower than perpendicular patterns. The pattern that retains water the longest is a maze pattern. The findings show that these patterns should not be neglected in peatland modelling as they have a strong effect on the hydrology and make peatlands more resilient to climate change. How strong this effect is should be studied further as the model used showed poor predictive power.

Contents

1 | Introduction

Peatlands cover ± 3 percent of the land surface on Earth of which most is located on the northern hemisphere (Nijp, 2015; Wieder and Vitt, 2006). Though the peat area is relatively small, it stores ± 30 percent of the global soil carbon (Gorham, 1991; Eppinga et al., 2009b; Wieder and Vitt, 2006). This carbon could be released into the atmosphere in the future due to global warming and thereby forming a positive feedback on climate change (Ise et al., 2008; Tarnocai, 2006).

Peat is defined as a soil which is formed by natural deposition of organic material from that same location (Rydin et al., 2013). If peat is still being formed it is called a mire which means that the vegetation for peat formation is present, and organic material is accumulating (Joosten and Clarke, 2002). In order for organic matter to accumulate, net primary production has to exceed organic matter decomposition, which results in CO_2 fixation in the soil (Moore et al., 1998; Vasander and Kettunen, 2006; Wieder et al., 2006). In peatlands this is reached by the slow decomposition of organic matter, which is primarily caused by a shallow groundwater table in combination with the low acidity and the characteristic slow decomposition of the plants (Laiho, 2006). Water reduces the decay in two ways: by decreasing the temperature of organic material and by the lack of oxygen present which is needed for decomposition (Joosten and Clarke, 2002). Peat consists mainly of mosses that undergo stress both at high and low water tables (Ridolfi et al., 2006). When conditions for peat formation persist over a long time period, peat increases in thickness (Vasander and Kettunen, 2006) and contains information on past vegetation and climate (Rydin et al., 2013).

The formation and persistence of peatlands is threatened by global warming, which will affect peatlands by means of a change in the water table and higher temperatures (Ferrati et al., 2005). According to the study by Gong et al. (2012) on peatlands in Finland, the increase in evapotranspiration with a 2 degrees Celsius temperature rise would need to be compensated by a 10 percent higher precipitation amount in order to maintain the same water level. Although an increase in precipitation is expected in Scandinavia, the events are projected to become more intense and less frequent (Allen and Ingram, 2002), causing larger water deficits for some time periods (Rydin et al., 2013). When water tables are lowered in peatlands, the aerated layer increases, which means that the peat will start to decompose and thus release CO_2 (Ise et al., 2008; Moore et al., 1998; Rydin et al., 2013; Whittington and Price, 2006). The study by Silvola et al. (1996) showed that a lowering of the average water table by 1 cm already increases the CO_2 emission.

Multiple studies suggest that peatlands may be resilient (defined as being able to remain functioning in the same manner) to climate change until a certain threshold is passed leading to a catastrophic shift (Eppinga et al., 2009b; Nungesser, 2003; Ridolfi et al., 2006; Rietkerk et al., 2004). A catastrophic shift is a sudden shift to a different ecosystem state which cannot easily be reversed due to hysteresis (Rietkerk et al., 2004). Spatial patterns in elevation and vegetation, that can often be found in peatlands, are said to be the first stage of this shift (Rietkerk et al., 2004). These patterns consist of hummocks and hollows, where hollows have a lower elevation and are closer above lowest water table (5-20 cm) than hummocks, which are higher (Rydin et al., 2013). Hummocks are usually between 1 and 3 meters in diameter whereas hollows are often larger (Baird et al., 2015). Different spatial organizations of hummocks and hollows can be found; on slopes, string patterns perpendicular to the slope (and groundwater streamlines) are found (Swanson and Grigal, 1988) whereas on flat areas maze or dotted patterns are found (see figure 1.1). The difference in pattern is caused by the surrounding/ local landscape and the anisotropy of the water flow due to feedbacks described later on (Eppinga et al., 2009b; Swanson and Grigal, 1988). The origin of these patterns is hypothesized by Eppinga et al. (2009b) to be initial peat formation which converts water flow in channels to sheet flow. The micro-topography then gets amplified since higher areas have faster peat accumulation, due to biomass feedbacks; vascular plants occur on the higher areas, which accumulate more biomass, resulting in an increasing elevation which again favours more vascular plant growth. With positive feedbacks this micro-topography grows into the patterns. This theory was already mentioned by Foster et al. (1983) who also explain enlargement of pools with standing water by means of faster decomposition due to oxygenated environments which enlarges and deepens the pool.

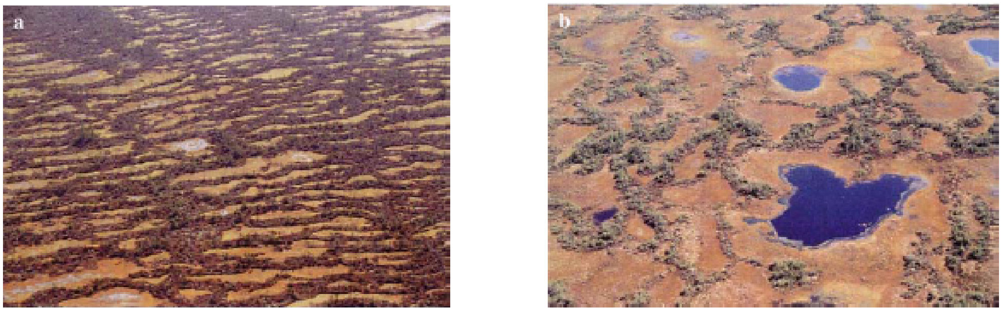

Figure 1.1: Examples of patterns that can be found in peatlands, from Eppinga et al. (2009b). Left: An example of a string hummock/hollow pattern on a slope. Right: An example of a maze hummock/ hollow pattern on a flat area

Once established, hummocks and hollows can be quite persistent through time by means of multiple feedbacks (Barber, 1981; Eppinga et al., 2009a):

- Feedback 1: Nutrients and biomass
- Feedback 2: Light availability, pH and temperature (not discussed in detail)
- Feedback 3: Water and conductivity

Hummocks have a higher elevation and are dryer than hollows, resulting in different plant species with a higher plant productivity and the occurrence of vascular plants (Rydin et al., 2006). The higher plant productivity makes sure the hummock remains or even increases its higher elevation, making it more suitable for vascular plants and thus again result in more biomass accumulation. The vascular plants on hummocks are able to accumulate nutrients by means of increased evapotranspiration and thus deplete the hollows (Eppinga et al., 2009a,b). This supports the suitability of hummocks for vascular plants, while making the hollows unsuitable for vascular plants. This feedback process contributes to the persistence of hummocks and hollows.

A very important feedback is water and conductivity. The vascular plants on a hummock have better capillary water transport, resulting in higher evapotranspiration which will lower the groundwater table. This will make the area more suitable for dryer vegetation types (Eppinga et al., 2009a; Rietkerk et al., 2004) and increase the maximum plant height (Verry, 1997). How much higher the evapotranspiration is on hummocks is not yet known. Heijmans et al. (2008) did provide crop factors for the evapotranspiration of hummock and hollow plant species, but other aspects such as the elevation difference and variation in groundwater level depth may be of importance. When the tree density on a hummock becomes higher, the strength of this evapotranspiration feedback may shift as the shadow provided by the trees will reduce soil evaporation and thus the water level increases (Limpens et al., 2014). Due to the spatial variation in vegetation (Baird et al., 2015), the underlying peat has a different structure resulting in a different hydraulic conductivity between hummocks and hollows (Loisel and Yu, 2013; Rydin et al., 2013; Yuan et al., 2015). The hydraulic conductivity describes how easy water can flow trough the soil medium (Boelter, 1965). Most studies have found the hydraulic conductivity to decrease with depth in peatlands, as the peat material gets more compressed and humified with depth (Branham and Strack, 2014; Boelter, 1965; Clymo, 2004; Rydin et al., 2013). The study by Baird et al. (2015) however, showed that in deeper peat, equal and even higher conductivities could be found than at the surface. They argue that this does not necessarily lead to water flow since a connectivity between high conductivity zones is needed for this. The variation in conductivity between hummocks and hollows, with hummocks having a lower conductivity, result in water storage upstream in hollows (Baird et al., 2015; Eppinga et al., 2009b; Ivanov et al., 1981; Loisel and Yu, 2013). This causes hollows to persist upstream of hummocks, given that hummocks are not probable to form on wet locations. It also determines the distance between hummocks and hollows since the distance between hummocks is optimized so that the negative feedbacks from a hummock do not influence the next hummock. Since most feedbacks act upstream, on a slope perpendicular strings of hummocks form (Swanson and Grigal, 1988). The variation in conductivity is not found at greater depths by the studies of Baird et al. (2015); Branham and Strack (2014), raising the question whether hummocks and hollows persist over depth or whether peat botanical composition has no influence on the conductivity any more at larger degrees of decomposition (Branham and Strack, 2014).

In wetlands the occurrence, shape and spatial organization of patterns are found to control the water discharge by means of their variation in hydraulic conductivity (Kaplan et al., 2012; Yuan et al., 2015). Yuan et al. (2015) found a clear link between pattern characteristics (of ridges and open water) and the amount of time a surface is covered with water. Areas with a high ridge (pattern form with a higher elevation) density inhibit the water flow resulting in water logging and thus wetter conditions for longer time periods (Eppinga et al., 2009a). Kaplan et al. (2012) found in a wetland system with open water with small islands, that the orientation and connectivity of ridges influences and is influenced by the flooding dynamics. These studies are performed on different structures than hummocks and hollows, but since they incorporate patterns with variation in the hydraulic conductivity, similar findings are expected in a peat system with hummocks and hollows.

Studies that use models to predict the effect of climate change on peatlands often do not incorporate the variation in hydraulic conductivity and evapotranspiration between hummocks and hollows (Gong et al., 2012). Most models use an acrotelm -catotelm approach with a fixed conductivity for the saturated and unsaturated part of peat (Belyea and Baird, 2006; Eppinga et al., 2009a). By neglecting the patterns and the effect their conductivity has on hydrology, the models could wrongly estimate the effect of climate change (Baird et al., 2015). The orientation, size and spatial organization of hummocks and hollows could affect the water retention within a peatland by means of blockages by for example hummock strings, which would lead to slower declines in the water table. Therefore the objective of this study is to find how the spatial organization of hummock and hollow patterns affect the hydrology in peatlands and thus the resistance to climate change.

1.1 Research questions

The objective will be reached through both field work and a model study. The main research question is:

- What effect does the hummock hollow patterning have on the hydrology of a peatland?

Various subquestions have been set up in order to answer this research questions. The subquestions that will be answered through field work and data analysis are:

- Is there a difference in saturated hydraulic conductivity between hummocks and hollows?
- How does the saturated hydraulic conductivity change over depth?
- Is there a difference in evapotranspiration between hummocks and hollows?

The subquestions that will be answered through a model study are:

- How does the distance between hummocks influence the hydrology?
- How does the orientation of hummocks and hollows influence the hydrology of a peatland?
- How does the spatial organization of hummocks and hollows influence the hydrology of a peatland?

1.1.1 Hypotheses

The hypothesis of this study is that the spatial organization of hummocks and hollows affects the hydrology of a peatland in such a way that string patterns result in more resilience to the expected dry periods with climate change. This would become evident when using various pattern scenarios in a model, where the scenario without a pattern would dry up the fastest. It is hypothesised that the hummock/hollow pattern affects the hydrology of a peatland in such a way that it is more resilient to the expected dry periods with climate change. The pattern expected to have most effect is the string pattern due to the long blockages which are more connected than for example a dotted pattern.

In order for the patterns to have an effect, a difference in hydraulic conductivity is expected to be found with hummocks having a lower hydraulic conductivity (Eppinga et al., 2009b; Loisel and Yu, 2013). The hydraulic conductivity is expected to decrease with depth as deeper peat is compacted through pressure of the overlying peat and is more humified (Branham and Strack, 2014; Rydin et al., 2013).

2 | Methods

In order to answer the research questions, a combination between fieldwork and modelling was used. In the field the hydraulic conductivity was measured at various locations and depths. Along with this the evapotranspiration was measured indirectly (see section 2.3.3). Furthermore peat samples were taken which were used to calculate the porosity which was needed as a model parameter and for data correction for the hydraulic conductivity measurements. By performing statistics on the obtained data the variation in hydraulic conductivity and evapotranspiration between hummocks and hollows was studied. The other questions were answered through a model study. This chapter describes the methods in more detail.

2.1 Study area

The study area selected for this study was Degerö Stormyr. It is positioned in the Kulbäcksliden Experimental Forest in Sweden at an altitude of 270 meters. This choice was based on the presence of various microform patterns and convenience since board-walks to reach the area were already present and various parameters, such as the precipitation, were being monitored continuously at the site.

In Degerö Stormyr the geology underneath the peat consists out of a gravelly sandy loam till on top of a bedrock of gneiss (Magnusson, 1994). During the quaternary, Sweden was entirely glaciated resulting in a remnant of till in the area. This till area was covered with peat at the lowest parts whereas weathering took place in the higher parts (a map of the geology is provided in appendix B). This resulted in soil formation of about 0.4 meter where often podzols were formed (Amvrosiadi et al., 2016). This could be seen on the locations with a higher elevation that occur in the area; no peat has formed here and a shallow soil was found on top of the till. It was assumed that negligible weathering occurred underneath the peat due to the lack of oxygen and slow water flow.

Degerö Stormyr is a mire area, meaning that peat is still being formed currently. The study by Nilsson et al. (2008) states that the peat depth is between 3 and 4 meters at most locations, but depths of 8 meters have been found. The oldest peat is ± 8000 years old (Nilsson et al., 2008). Degerö Stormyr is topogenous, meaning that it is fed both by rainwater and groundwater (Wiedermann et al., 2009a). The catchment is mainly drained by a small creek in the north west. The average water table level measured over the growing season of 12 years is 14.1 cm below the surface (Peichl et al., 2014). The mean annual precipitation is 523 millimetres and the mean annual temperature is 1.2 degrees Celsius, based on 30 years (Alexanderson et al., 1991). The area is covered with snow from November till late April, resulting in a growing season from May until October. The vegetation consists mainly of sphagnum species where the hummocks were dominated by *Sphagnum fuscum* and the hollows by *Sphagnum majus*. *Sphagnum balticum* is also often found in lawns and hollows (Wiedermann et al., 2009b). The vascular plants that occur on the hummocks were *Eriophorum vaginatum*, *Trichophorum cespitosum*, *Vaccinium oxycoccos*, *Andromeda polifolia* and *Rubus chamaemorus* (Peichl et al., 2014).

The study site has board-walks that made it possible to reach hummock and hollow areas (see figure 2.1). Six measurement sites were selected in the field based on the presence of hummock hollows patterns, the location in the mire and the accessibility. At site one and two (figure 2.1) extra board walks were installed so two hummocks and two hollows could be reached. At each measurement site a relatively large and a relatively small hummock hollow pair were selected, resulting in four measurement locations per site. The different sizes of the hummock and hollows were selected because of the possible effect of the pedological memory; in the past the micro-forms could be a hollow instead of a hummock or the other way around. This effect was expected to be larger in smaller micro-forms, as the feedback mechanisms have less effect. This might have an effect on the hydraulic conductivity. This phenomena was not used for this study, but for a simultaneous study by Westrene (2017). Four extra locations were selected in order to get a better measurement coverage of the mire (see figure 2.1). Two locations were used for reference measurements (see section 2.2.1).

2.2 Measurements

Fieldwork was conducted from 20-06-2016 till 20-07-2016 in the study area described above. This period was chosen based on the accessibility of the mire, working conditions and convenience. A description of all the measurements and observations made in the field were described in this section.

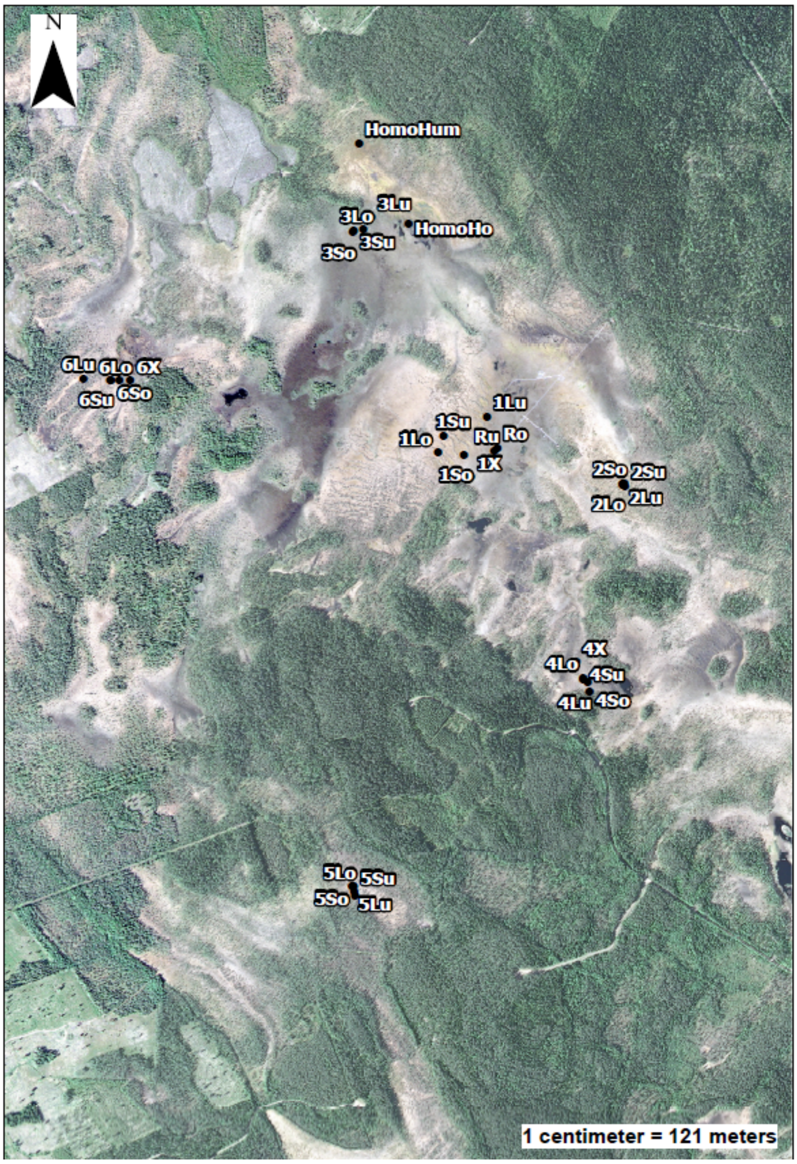

Figure 2.1: Study site with the measurement locations (black dots). Each location has a code which starts with the board walk number, followed by either a L (large) or a S (small) and an u (hummock) or an o (hollow). The extra locations received the code of their board walk with a X (extra) or the abbreviation for homogeneous hummock or hollow (HomoHum or HomoHo). The reference measurements start with a R

2.2.1 Hydraulic conductivity

The hydraulic conductivity was measured in the field by means of a slug test at various depths. During the slug test water was added to a piezometer. With the water table draw down after the water addition, the hydraulic conductivity was calculated.

For the slug test a piezometer was made with an outer diameter of 4 cm and a filter of 10 cm at the bottom. The filter made sure the piezometer was in contact with the groundwater and thus enabled water to flow in and out of the piezometer. The piezometers were made out of plastic tubes in which a filter was created by drilling 104 holes with a diameter of 8 mm over the length of 10 cm, which were 7 cm above the bottom of the tube for firmness. This resulted in a filter with a perforation rate of 41.6 %. The bottom of the piezometer was closed watertight with a lid. The filter was protected against clogging with a stocking which was placed over the filter; this allows water to flow through and prevents smearing. Smearing can cause an underestimation of the hydraulic conductivity, because the soil in the filter results in reduced flow (Baird et al., 2004).

The piezometer was inserted in a pre drilled hole by a gouge with a slightly smaller diameter than the piezometer.

The depth at which it was inserted was determined by using a device that beeps as soon as it touches water, attached to a tape-measure. With this device the groundwater level was measured, after which the piezometer could be placed at the correct depth. All measurements were performed below the groundwater table since the methods used were only valid under saturated conditions. The water table was used as reference so the surface elevation difference between hummocks and hollows had no effect and to make sure the first measurement of 10 cm was below the water table. The measurement scheme was based on the expected exponential decrease in hydraulic conductivity over depth. The depths were chosen beforehand, based on the estimated stabilization time, at 10, 30, 60, 100, 150, 200, 250, 300, 350 and 400 cm below the groundwater table. Due to time restrictions and longer stabilization times than anticipated, most locations were only measured till 100 cm. In total, 138 hydraulic conductivity measurements were performed (for more details on measurement amounts and depths, see Appendix C).

A diver was placed inside the piezometer that measured the water pressure at a time interval between 5 and 15 seconds, based on the measurement duration (Baird et al., 2015). Multiple divers of the type TD Divers DI240, Van Essen Instruments and Level TROLL 700, were used to conduct measurements simultaneously. After piezometer placement, the water inside the piezometer was allowed to stabilize (Baird et al., 2004). The time needed for this stabilization depends on the hydraulic conductivity (Hvorslev, 1951), so this time was estimated beforehand based on literature and previous measurements. When the water had stabilized, 100mL of water was poured into the piezometer. This amount was chosen since adding large amounts of water could result in unrealistic pressure gradients, possible erosion, possible turbulent flow and swelling of the surrounding peat which would have an effect on the hydraulic conductivity (Baird et al., 2004). Adding less water would result in a smaller peak, making the calculations more difficult. Furthermore Hvorslev (1951) stated that the volume of flow required for water level stabilization should be small to increase the sensitivity of the measurements to rapid pressure changes. After adding the water, the piezometer was left to stabilize again whilst the diver measured the decline in water pressure over time.

Reference hydraulic conductivity

Peat can swell and shrink caused by the amount of water present in the soil. The amount of shrinkage can be quite substantial; the study by Nijp (2015) found a seasonal surface elevation difference of 8 cm in Degerö Stormyr. As the hydraulic conductivity is influenced by soil compression due to smaller pore space, a decline was expected in dryer periods. This is a self-preservation process of the peat, as a lower conductivity results in longer travel times of water through the soil and thus the soil will remain waterlogged (Price, 2003). This was not studied in this thesis, but as the swelling and shrinking has an effect on the hydraulic conductivity (Baird et al., 2004) it was accounted for by means of reference measurements.

Two piezometers were used to monitor the change in hydraulic conductivity through the fieldwork period. One was placed in a hummock, the other in a hollow at a depth of 30-40 cm below the groundwater table, as this is the depth where most shrinkage occurs (Schlotzhauer and Price, 1999). By using only two piezometers the assumption was made that swelling and shrinking is homogeneous for all hummocks or hollows. This assumption was made since the focus of this study was not on this process and the rest of the divers was needed for the other measurements. The conductivity was measured on a daily basis at the two sites, resulting in data of the hydraulic conductivity in time. If a clear relation between the groundwater level and hydraulic conductivity was found, the conductivity measurements were corrected for this with the groundwater level during the measurement.

2.2.2 Samples and vegetation

In order to correct the hydraulic conductivity measurements for groundwater level changes (see section 2.3.2), peat samples were taken from all locations and depths where the hydraulic conductivity was measured. For this study those samples were used in order to determine the porosity of the peat. This was done by determining the bulk density and particle density in the lab. These samples were also used for a simultaneous study on macro-fossils by Westrene (2017). The peat samples were taken with a Russian corer with a diameter of 4.5 cm. A section of 2 cm was cut from the soil core, starting at the top of the filter depth (e.g. from 10 to 12 cm). These samples were taken after the hydraulic conductivity measurements were finished in order to not influence the measurements by disturbing the soil. The vegetation at each measurement site was observed within 4 classes: moss, trees, dwarf shrubs and sedge. This was done to calculate the evapotranspiration, which differs for each of the classes (see section 2.4.1). For a surface of 1 m^2 the percentage of coverage for each class was noted.

2.2.3 Evapotranspiration

Since evapotranspiration can be dependent on the vegetation type (Brümmer et al., 2012), a difference in evapotranspiration was expected between hummocks and hollows (Eppinga et al., 2009a; Rietkerk et al., 2004). Evapotranspiration was measured at the field site with an eddy-covariance set-up (Aubinet et al., 2012). This set-up has a footprint of $\pm$ 200 squared meters that typically overlaps with a hollow. In order to quantify the small scale variation between hummocks and hollows, measurements were performed with an infra-red camera (Jones, 1977; Maes and Steppe, 2012; Moffett and Gorelick, 2012). Since evaporation costs energy, variation in surface temperature indicates variation in evapotranspiration (Maes and Steppe, 2012). Seguin et al. (1982) showed that this method should not be used for predicting absolute evapotranspiration values, but proves valuable for studying spatial variations. The method used to calculate evapotranspiration was proposed by Jackson et al. (1977), who found an expression that relates evapotranspiration to net radiation (R_n), air temperature (T_a) and canopy temperature (T_c):

$$ET = R_n - B(T_c - T_a) \tag{2.1}$$

where B is a site dependent composite constant, consisting out of the wind speed, soil heat flux and the volumetric heat capacity of air. The canopy temperature was measured by taking infra red photo's. The camera used for the photo's was the FLIR ONE for Android, which is a small camera that can be plugged into an android phone. In combination with the FLIR ONE application, infra red photo's were taken with an accuracy of $\pm$ 2 degrees Celsius (Allain, 2014). The net radiation and air temperature were measured by the meteorological station present in the field.

The infra red photo's were taken at the measurement sites of the hydraulic conductivity, since these contain either hummock and hollows, water table measurements were taken here to establish a relation with evapotranspiration, and the piezometer could be used as a reference point in the pictures. To make sure the same area was photographed each time, small plastic tubes were inserted in the peat, creating a frame of 70 by 80 cm (see figure 2.2). Since the photo's could be influenced by meteorological conditions, they were taken around the middle of the day, preferably under cloudless conditions. If this was not possible a day was skipped or all sites were photographed under cloudy conditions. During each measurement day an additional photograph was taken of the reference site, which was the footprint of the meteorological station. This was done in order to calibrate the calculated evapotranspiration with the one measured with the eddy-covariance set-up, and to determine the constant B. The constant B could be derived as the actual evapotranspiration value is known at the reference site and all other parameters were measured. In total, 134 infra red pictures were taken over 8 different days (for more information on the conditions and number of measurements per microform see appendix C).

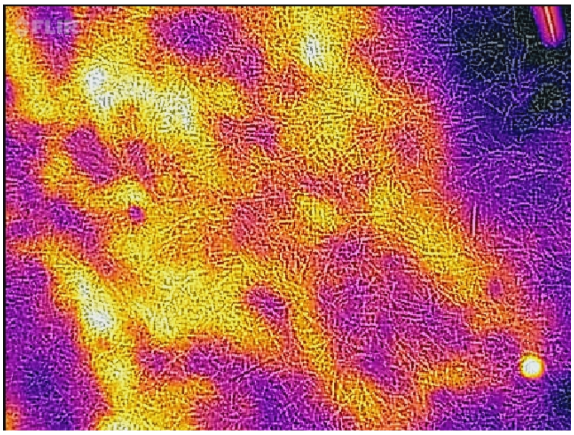

Figure 2.2: Example of one of the infra red photo's taken. The piezometer can be seen in the top right, and the reference frame can be seen at the bottom right (light circle). The highest temperature in the figure is 15.2 degrees Celsius and the lowest temperature is 5.8 degrees Celsius

2.3 Analysis

2.3.1 Porosity

The porosity of the peat, which was needed for the diver correction for groundwater level changes and the model study, was determined in the lab by measuring the bulk density and the particle density. The particle density was calculated as $P_d = W_d/V_s$, where P_d is the particle density, W_d is the dry weight of the soil sample and V_s is the soil volume which is measured by the pycnometer. The porosity ρ was calculated in percentage as: $\rho = 100 - (B_d/P_d) * 100$, where B_d is the bulk density (Eijkelkamp, 2012). The bulk density was measured by weighing the peat samples after drying them in the oven at 70 degrees Celsius for 48 hours. The protocol for determining the bulk density states that the soil should be dried at 105 degrees Celsius (Alterra, 2013; Blake, 1965). This protocol was not followed since at 105 degrees the organic material in the peat may start to burn (Nijp, 2015). With the known volume of the sample and the dry weight, the bulk density was calculated. The particle density was measured by means of an air pycnometer (figure 2.3). This device measured the volume of a sample, which together with the weight of the sample leads to its density. The volume was measured by putting the sample in an airtight chamber after which the mercury was pumped up. The switch was then turned from pumping to measuring and the mercury level decreased until it was stabilized at the level which shows the volume of the soil sample on the left hand side (Alterra, 2013).

Figure 2.3: Pycnometer used for the porosity calculations. The air tight chamber is behind the black knob, the pump can be seen on the right and the switch on the left (red)

2.3.2 Hydraulic conductivity

Data correction

As divers measure pressure, not only the water column above but also the barometric pressure has an effect. Fluctuations in barometric pressure could produce noise or a trend in the pressure measured by the diver, especially for the more time consuming measurements in deeper peat layers. Therefore the barometric pressure needed to be measured alongside the hydraulic conductivity (Greswell et al., 2009). The barometric pressure was obtained from the meteorological station present in the study area where it was measured with a time interval of one minute. It was then subtracted from the pressure measured by the divers. Other disturbances in the hydraulic conductivity measurements could be caused by changes in groundwater level during a measurement other than caused by the slug test. A change in groundwater level could be caused by precipitation, evaporation and runoff. Data from the meteorological station on evaporation (30 minute interval) and precipitation (15 minute interval) was used to correct the divers for this with use of the porosity. The measurements were not corrected for runoff. The measured evaporation by the eddy covariance tower was applied to all hummocks and hollows, though the footprint of the tower consists out of solely hollows (see section 3.4). The porosity was calculated as described in section 2.3.1.The same porosity value was used for all depths and locations (see section 3.1). The value 0.927 was used which is the average porosity for the depths between 10 and 20 cm. This was done since the fluctuations in the groundwater level took place in this region. The divers were then corrected by:

$$P = P_i - P_{air} - ((R - ET)/\rho), \tag{2.2}$$

where P is the corrected diver pressure in hPa, P_i is the initial diver pressure in hPa, P_{air} is the barometric pressure in hPa, R is the amount of precipitation in mm, ET is the amount of evaporation in mm and ρ is the porosity. This corrected diver pressure was used for further calculation of the hydraulic conductivity.

Calculation

Prior to the actual hydraulic conductivity calculation, a section of the diver data was selected. The calculations started at the water addition and ended when the pressure returned to its original value (see figure 2.4). If the pressure did not return to this value (e.g. due to a groundwater rise that was not corrected for or due to the piezometer being installed at a deeper level prior to stabilization), the end point was determined by hand. After this the selected curve was normalized, and the conductivity was determined on the normalized head range (Butler Jr, 1997) from 0.07 to 0.8, in order to prevent disturbances in the top and the tail of the peak to influence the calculations.

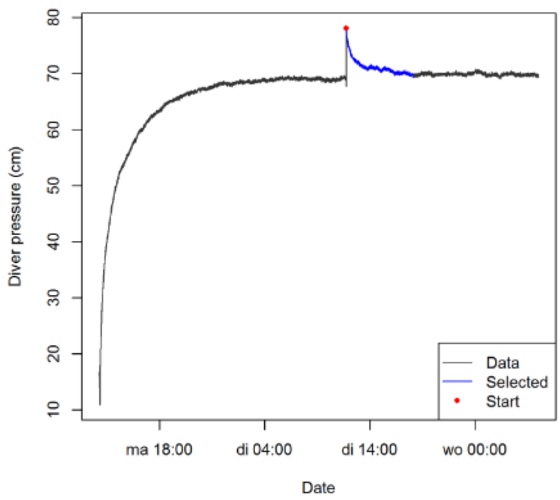

Figure 2.4: Example of the water level response to a slug test : the peak shows the result of the water addition. The red dot is the starting point of the curve. And the blue line is the entire curve on which the calculations were performed. The rise in pressure which can be seen in the beginning is the stabilization curve after piezometer installation

For this study the method by Bouwer and Rice (1976) was used, based on the study of van Dijk et al. (2016) who compared various slug test analysis methods and found Bouwer and Rice (1976) to be the most suitable. van Dijk et al. (2016) used this method in combination with the Zlotnik shape factor which accounts for piezometer geometries (Zlotnik et al., 2010). There were multiple methods to determine the hydraulic conductivity, such as Beers (1983); Bouwer and Rice (1976); Hvorslev (1951). The method by Beers (1983) is for calculations over an entire aquifer by means of an open hole instead of a piezometer. Since this was not the used method for this study, this method was not used. Bouwer and Rice (1976) can be applied for party penetrating wells, whereas Hvorslev (1951) was designed for fully penetrating wells. Bouwer and Rice (1976) found that the method by Hvorslev (1951) leads to a large error when executed near the groundwater table since it assumes a confined aquifer. The rigid soil theory was used since a small amount of water was added, thus no swelling and shrinking of the peat was expected because of the water addition (Baird et al., 2015; Holden and Burt, 2003).

The R script created for the study of Nijp (2015) was used as basis for the calculations. The study by Nijp (2015) used the formula developed by Bouwer and Rice (1976) who used the Thiem equation for steady state flow to or from a well to create an approach suitable for partly penetrating wells in confined and phreatic unconfined aquifers.

The formula used is:

$$Q(t) = 2\pi K_s L \frac{h(t)}{F} \tag{2.3}$$

where $Q(t)$ is the flow rate to or from the well, K_s is the saturated hydraulic conductivity, L is the filter length, $h(t)$ is the change in water level in the well relative to initial groundwater level, and F is a shape factor correcting for the geometry of the well (Nijp, 2015). The shape factor used was calculated by the expression of Zlotnik et al. (2010):

$$F_{ZGD} = \left(\sum_{i=1}^{\infty} \left\{ \left(cos(\beta_i \frac{H}{D}) - cos(\beta_i \frac{H-L}{D}) \right)^2 \frac{K_0(\frac{\beta_i r_w}{D})}{\beta_i^3 K_1(\frac{\beta_i r_w}{D})} \right\} \right) \Big/ \frac{L r_w}{2D^2} \tag{2.4}$$

where β_i is $\pi(i-0.5)$, H is the distance from the top of the aquifer to the bottom of the filter, D is the aquifer thickness, L is the filter length, K_0 and K_1 are the Bessel functions and r_w is the well radius corrected with the anisotropy ratio (the ratio between horizontal and vertical hydraulic conductivity) which was assumed to be 1 (Nijp, 2015; Zlotnik et al., 2010).

During 15% of the measurements it occurred that the water was added while stabilization had not yet been completed. This resulted in an increase in pressure after the water was added (see figure 2.5). Since the hydraulic conductivity could not be calculated using the method described above, an unconventional method was used. Instead of calculation the hydraulic conductivity after adding water, it was calculated from the pressure rise after piezometer installation till the start of the slug test. The data obtained through this method was interpreted with caution since the large pressure head difference can lead to errors (Baird et al., 2004; Hvorslev, 1951).

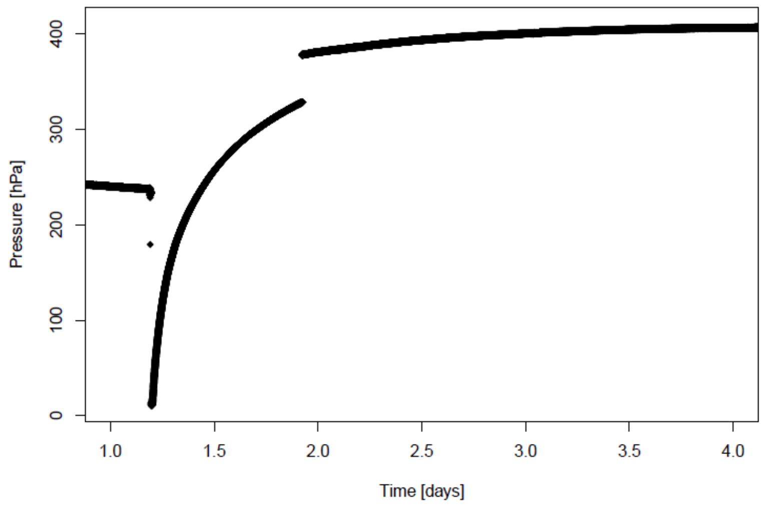

Figure 2.5: An example of a case where water was added prior to stabilization completion. This can be seen from the increasing pressure after the water addition

First the pressure curve was selected from the piezometer installation till the water addition. On this part a formula was fitted with the form of an exponential variogram;

$$Pressure = a\left(1 - exp\left(-\frac{x}{b}\right)\right) + c. \tag{2.5}$$

Since the stabilization was not yet complete, the full curve on which the hydraulic conductivity was calculated was predicted using the fitted parameters. The full curve was then reversed in order to get the same type of curve as with the other conductivity calculations. The rest of the calculations were the same as the ones calculated on the slug tests.

Statistics

First the reference measurements on the effect of peat swelling and shrinking were studied on whether a correlation between the hydraulic conductivity and the groundwater level occurred. This was done by using a Pearson correlation.

A significant correlation would result in correction for the hydraulic conductivity values for the groundwater level at the time of the measurement. Second it was tested whether the hydraulic conductivity varied significantly between hummocks and hollows in a visual manner. A function was fitted through the hydraulic conductivity values found in the field, averaged for each depth. The average was taken to account for the variation between the measurements, possibly caused by location in the catchment, hummock or hollow size and other local variabilities that were not accounted for in this study. The function was fitted for hummocks and hollows separately in R with the package nls2. The form of the fitted function was:

$$K = a * e^{-b*D} + c, \tag{2.6}$$

where a, b and c are the fitted parameters, K is the hydraulic conductivity in md^{-1} and D is the depth in cm. The form was based on the shape of the measured hydraulic conductivity values over depth. The root mean square error was used to assess goodness of fit. After fitting functions for hummocks and hollows the 5% and 95% intervals of the parameters and thus function were calculated and plotted together. When hummocks and hollows vary significantly, the functions and their intervals will not overlap.

2.3.3 Evapotranspiration

Calculation

In order to extract the canopy temperature from the infra red pictures the program BFIC (EEVblog Electronics Community Forum, 2013) was used. The images were cropped with 48 cells (of 240 x and 320 y cells) to remove disturbances. The average temperature was used as canopy temperature for further calculations.

The net radiation and air temperature, which were measured by the meteorological station, were averaged over 4 hours; 2 hour previous to the infra red picture, and 2 hours after. This was done to cancel out extreme values that can occur during momentous measurements. The constant B was derived from the reference site (see section 2.2.3) from the evapotranspiration measurements taken under sunny conditions. This was done so the difference between the air and canopy temperature would be the largest, so the relative error of measurement errors would become smaller. For the evapotranspiration calculations it was assumed that B was equal for hummocks and hollows and remained the same under various meteorological conditions. The difference in evapotranspiration between hummocks and hollows was then caused by the difference in canopy temperature and net radiation.

The net radiation will differ between hummocks and hollows by means of a difference in the albedo. The incoming radiation was assumed equal over the entire catchment, but the amount of reflection was assumed to differ. The albedo was determined from meteorological station in combination with literature. The albedo of the hollows was measured at the meteorological station and thus was already available. Yazaki et al. (2006) found that the albedo of hummocks was 0.028 than for hollows. With these albedo's the net radiation was calculated.

Since T_c was measured at a single time during the day, the evapotranspiration was calculated as mm per hour, and was only valid for the middle of the day. This was done to prevent an overestimation of evapotranspiration that would occur when T_c was assumed to be equal throughout the day.

Statistics

The data was tested for normality with the Shapiro-Wilk test in SPSS. Then the calculated evapotranspiration for the hollows was compared with the observed one. This was done in order to validate the used method of infra red imagery. Only hollows were used since the eddy covariance tower had a footprint consisting solely out of hollows. In order to test whether the calculations were the same as the observed values, the paired t-test in SPSS was used (Lund Research Ltd , 2013). Each calculated evapotranspiration value was paired with its corresponding observed value. By using pairs the bias of the groundwater and time of the measurement were removed Rubin (1973). With this test it could be determined whether the infra red method was significantly different form the observed values and whether it was a good predictor for the absolute value of evapotranspiration.

To test whether the evapotranspiration rate was significantly different between hummocks and hollows a paired t-test was used. By doing this the relationship was studied which could be used in the pattern scenario model. The paired t-test was used to account for the effect of the groundwater and time. The pairs were matched per location site and thus time as one site was measured in approximately 5 minutes. The large hummock was then paired with the large hollow, and the small hummock and hollow were paired. This was done in case size of the hummock or hollow has an effect. Finally, a linear regression was performed on the evapotranspiration data and the groundwater level to find out whether the groundwater level can predict the evapotranspiration.

2.4 Geohydrological model

The effect of the distance in between hummocks and hollows, the spatial organization and orientation of the patterns on the hydrology of a peatland was studied through a geohydrological model. The effects of various patterns on the hydrology were studied by applying a precipitation event to a domain within the Degerö Stormyr catchment, after which no further precipitation occurred. The peak response and states of the groundwater level showed how various patterns responded to this event and the following drought. The model was made in R with use of a package created by Paul Torfs called FVFE2D. The decision for using this finite volumes and finite elements package are based on the non-linearity of the fluxes in the model (such as the hydraulic conductivity function), the large spatial variability that requires a spatial variable grid size (section 2.4.3) and the mass balance which is important for the model. The state this model calculates is the hydraulic head (H).

At first the aim was to model the entire Degerö catchment to provide in- and out-flux to a smaller domain. The catchment model was less detailed. It did not contain hummocks and hollows, but it did have differences in geology and vegetation. At some locations there was no peat and the till was at the surface, with forests on top. This resulted in variations in hydraulic conductivity and evapotranspiration. By using this model the groundwater flux during and after the event could be used as input for the smaller domain, giving more realistic boundary condition values. However, this catchment model had a too large run time (at least 2 months) since some instabilities were still present in the model causing a high number of iterations. Due to time constraints it was decided to not use this model, and only make use of the small domain. More information of the built up on the catchment model and the problems that arose can be found in appendix A.

2.4.1 Parametrization

Evapotranspiration

The results on evapotranspiration from the infra red camera could not directly be used for the model (see section 3.4). Instead a reduction function was used to calculate the evapotranspiration, since evapotranspiration can be limited by a lack of water and low groundwater levels were present in the model runs. This reduction function depended on the vegetation type, as some plants stop evaporating at a shallower groundwater table than others (Mezbahuddin et al., 2016). The reduction function used was as follows:

$$\begin{aligned} &ET = k * ET_{pot} && (state > D_{opt}) \\ &ET = k * ET_{pot} * \frac{(state - D_{opt})}{D_{opt} - D_{min}} && (D_{opt} > state > D_{min}) \\ &ET = 0 && (state < D_{min}), \end{aligned} \tag{2.7}$$

where ET is the evapotranspiration, ET_{pot} the potential open water evapotranspiration,k is a crop factor, D the depth of the groundwater level and opt and min are the optimum and minimum level for evapotranspiration respectively. The evapotranspiration was calculated per plant species group (graminoids, ericacious, sphagnum hollow and sphagnum hummock) after which the sum was taken based on the fraction of occurring plant species estimated in the field as % cover, averaged for hummocks and hollows separately. This was done since more vascular plants occurred on hummocks which can evaporate until a lower groundwater level than the maximum groundwater depth for evapotranspiration in hollows, thus creating a difference in evapotranspiration between hummocks and hollows over groundwater level depth. The used vegetation fractions were estimated on 1 m^2 and averaged for hummocks and hollows separately No trees were found. Both hummocks and hollows contained mostly peat mosses. Hollows also had about a quarter of graminoid coverage, whereas for hummocks this was ericacious. The fractions from table 2.1 were used as model inputs for the evapotranspiration calculation.

The crop factors and values for the optimum and minimum groundwater level were based on Heijmans et al. (2008). The open water evapotranspiration was calculated with Penmann-Monteith with the available 30 minute interval meteorological data as input;

$$ET_{pot} = \frac{0.408 * S * (Rn - G) + \gamma * \frac{18.5}{t_{mean}+273} * ws * (es - ea)}{S + \gamma}. \tag{2.8}$$

Table 2.1: The vegetation cover in fractions for hummocks and hollows averaged.

Pattern entity	Ericacious fraction	Graminoid fraction	Moss fraction
Hummock	25	9	66
Hollow	2	24	74

S is the saturated vapour pressure in kPa, Rn is net radiation in Wm^{-2}, G is the ground heat flux in Wm^{-2}, γ is the psychometric constant in kPa^oC^{-1}, t_{mean} is the average temperature in ^oC, ws is the wind speed in ms^{-1}, es is the vapour pressure at the water surface in mb and ea is the vapour pressure in the atmosphere in mb. The ground heat flux was not measured in the field, but could be estimated as $0.05 * R_n$ (Kalma and Jupp, 1990).

Porosity

In order to built a transient model, the storage change at each time step was needed. The change in state depends on the porosity. The porosity was implemented as a function over depth, which was the same for the entire domain (see section 3.1). The depth-function was obtained from the field measurements.

Hydraulic conductivity

Hummocks and hollows have different parameters in their function of hydraulic conductivity over depth, see section 3.2. These different parameters were incorporated in the model based on the pattern scenario. Having a sharp boundary between hummocks and hollows and thus in the hydraulic conductivity led to instabilities in the model. At a node close or at a border, the value of the hydraulic conductivity may shift between iterations, causing the model to need the maximum amount of iterations (which was set at 500). In order to prevent this, a smoothing function was implemented. A buffer of 0.5 meter was placed around the hummocks, where the value inside a hummock was 0 and 1 for a hollow. In the buffer a linear function was made from 1 to 0 over the 0.5 meter. The transmissivity was then defined as: $kD = f(x,y) * kD_{hollow} + (1 - f(x,y)) * kD_{hummock}$, where $f(x,y))$ is the function including the buffer that shows whether a location in at a hummock or a hollow. The function of k has the form $k = a * x^{-b}$, where x is the depth. In order to get the kD the integral of k was taken over the saturated part of the peat profile. This led to the function:

$$kD = \frac{a * D_{peat}^{(1-b)}}{1-b} - \frac{a * D_{GWL}^{(1-b)}}{1-b}, \tag{2.9}$$

where a and b are estimated parameters and D is the depth of either the peat or the groundwater level (GWL). D_{peat} is a constant as the peat depth was set at 4 meter in the model.

The hydraulic conductivity was implemented in the model through the Darcy groundwater flow equation: $Q = -kD * \frac{dH}{dx}$, where Q is the groundwater flow in m^3d^{-1}, kD is the hydraulic conductivity integrated over the depth of the aquifer and $\frac{dH}{dx}$ is the gradient of the groundwater level. The model was not made to include open water flow; when the water level became higher than the peat surface, the excess water was removed and the groundwater level was set at the surface level.

2.4.2 Technical aspects

In the model, the state depends on various fluxes (e.g. evapotranspiration), while these fluxes also depend on the state. In order to be able to do this with general functions, a complex solving technique was required. The model made use of the Newton-Raphson method to find a solution for the state. Newton-Raphson uses derivatives and calculates the solution in an iterative manner. As the derivatives are not directly implemented in the model, this can cause instability or the need for many iterations. This was the main reason the catchment model was not used, as the large number of iterations resulted in a runtime of at least 2 months. By smoothing various functions, the model needs fewer iterations and can drastically decrease the run time. The microforms were smoothed in the model by introducing a buffer, so no sudden shift between hummock and hollow occurred. By doing so, the evapotranspiration and hydraulic conductivity functions were also smoothed as they depend on the microform. In the scenario model only the peat was modelled, so less smoothing was needed over depth than for the catchment model, as this included various geological layers.

2.4.3 Set up

Domain

A domain of approximately 100 by 70 meter was selected within the Degerö catchment. This size was chosen to make sure that the patterns could be implemented (e.g. various strings could be present in a string pattern), but it remained small enough to be modelled in detail without having large run times. The domain was selected near the meteorological station, as meteorological data and groundwater levels were measured here, and a string pattern was present (see figure 2.6). The presence of this pattern enabled the use of no-flux boundaries. As string patterns are often described to occur perpendicular to the stream direction, a boundary parallel to the stream direction, thus perpendicular to the string pattern could be made. This means that groundwater will flow parallel to the boundary and not cross it. The other two sides of the domain were selected parallel to the string pattern. The total area of the domain was 7212.9 m^2.

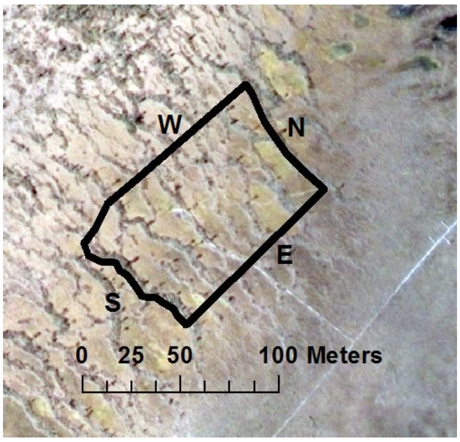

Figure 2.6: The selected domain, drawn by following the string pattern and thus streamlines. It is located near the centre of the mire at a board walk (white line). The sides of the domain are marked N,E,S,W for North, east, South, West respectively

Geology

As described in section 2.1 the geology consists out of till with a peat layer on top. For the model, only the peat layer was taken into account. It was assumed that at this scale the till layer does not significantly affect groundwater flow. The assumption was that there was no vertical flow, and that the amount that flows into the domain through the till layer was the same amount that flows out the domain through the till layer. When modelling at a larger scale the till layer will have an influence, thus it was incorporated in the catchment model. The peat layer was set at 4 meters, as at most areas the depth is between 3 and 4 meters Nilsson et al. (2008). More detailed measurements on peat depth are being executed in the area by using a ground penetrating radar, but were not yet suitable for use in the model at this stage.

Boundary conditions

The East and West side of the model were no-flux boundaries. The North and South sides had a Cauchy boundary condition. This means that the in- and outgoing flux were not known and had to be estimated based on the hydraulic head at the boundary (see equation 2.10).

$$Q = \frac{H_x - H_{BC}}{kD(H) * \Delta x}, \tag{2.10}$$

where Q is the flux over the boundary determined by the gradient of the hydraulic head between the boundary H_{BC} and a point 100 meter (Δx) away (H_x), and $kD(H)$ is the hydraulic conductivity at the boundary. The hydraulic conductivity was calculated at the boundary, depending on the current hydraulic head and microform. The point 100 meter away was chosen by hand in ArcMap from which the elevation gradient over the 100 meters was extracted from a smoothed DEM. As the boundary was not a point but a line, the average elevation was calculated and used. The North and South boundary both consisted of multiple lines (North of 7, South of 15), so the average was taken for each line segment separately

Initial condition

In order for the model to run, an initial groundwater value relative to the surface was needed. The initial plan was to use the catchment model for this, so the initial values would be varying in space. As the model could not be used, field measurements were implemented. The groundwater level was, however, only measured at one location, approximately 200 meters from the domain. Therefore the initial condition was set the same for the entire domain. The groundwater level at the start of the period of the used meteorological data was implemented, which was 27.86 cm below the peat surface on 9-7-2006. The initial condition was then the elevation at each location minus the groundwater depth. After each time step the calculated groundwater levels were set as the new initial condition for the next time step.

Digital elevation model

One of the inputs of the model was the digital elevation model (DEM). The elevation was needed to calculate ground water depths at each node and in order to have the peat surface gradient which together with the groundwater level influenced the water flow. The DEM used had a cell size of 2 meters. Since the chosen domain in reality has a string pattern (figure 2.6), this could be seen in the DEM. In order to study various patterns, the original patterns should not have an influence through the elevation difference. Therefore a smooth version of the DEM was created by averaging the surface elevation with a radius of 20 meters, thus removing the small local deviations.

Period selection and precipitation event

Meteorological data was available from 2000 till 2010 with half hour intervals. This data was needed for both realistic precipitation events and potential evapotranspiration values. The precipitation was measured with a tipping bucket (mm) and the evapotranspiration as latent heat flux (W m^{-2}) with an eddy covariance tower. A drought was selected within the growing season (May till October) as no snow was present in this period. The selected drought occurred in 2006 (Peichl et al., 2014), which lasted from 9-7-2006 till 14-8-2006. Some missing values were present in the data, but no large gaps occurred, so the average of the half hour before and after was taken. Previous to the drought there was a precipitation event of 7.8 mm. Since precipitation events are expected to become more extreme, and in order to see a clear effect in the model, a larger event was selected. Based on Nijp et al. (2016) a rare extreme event is larger than 40 mm. The event closest to 40 mm in 2006 was 47.6 mm in one day. This event caused an estimated water level rise of 10 cm (estimated from the groundwater level time series), so had a clear effect without rising above the surface level (the 10 cm was a rough estimate since it depends on the current water level, as porosity varies over depth). The groundwater level responds quite quickly to precipitation. By studying large events in 2006 it was found that the peak in groundwater level passes after approximately 7 days. Therefore it was assumed that the drought duration and thus maximum runtime of 37 days would be sufficient to study the entire peak passage.

Patterns

In total 9 different patterns were modelled. The patterns were either taken directly from an existing pattern on the aerial photograph of Degerö Stormyr in ArcMap (pattern StringReal, StringOrient, MazeReal, MazeOrient and DottedReal) or were altered in R or ArcMap. The modelled patterns and their used abbreviations were:

1. Homogeneous hummock (HomHum)
2. Homogeneous hollow (HomHol)
3. String pattern perpendicular to the flow direction (StringReal)
4. String pattern parallel to the flow direction (StringOrient)
5. Buffer of 1 meter around the hummocks of pattern 3 (StringBufHum)
6. Buffer of 1 meter around the hollows of pattern 3 (StringBufHol)
7. Maze pattern perpendicular to the flow direction (MazeReal)

8. Maze pattern parallel to the flow direction (MazeOrient)
9. Dotted pattern (DottedReal)

Table 2.2: The pattern scenarios and their names as they are used in the text. The reason for which a pattern is used is marked with an x and can be on the various pattern types, the orientation (parallel or perpendicular) of the pattern, the distance between hummocks/ hollows and the difference between hummocks and hollows (for the homogeneous scenarios).

Scenario number	Scenario name	Used to test the hypothesis about:			
		Pattern type	Orientation	Distance between microforms	Difference hummock/hollow
1	HomHum	x			x
2	HomHol	x			x
3	StringReal	x	x	x	
4	StringOrient		x		
5	StringBufHum			x	
6	StringBufHol			x	
7	MazeReal	x	x		
8	MazeOrient		x		
9	DottedReal	x			

By using these patterns the effect of various patterns, their orientation and the distance between hummocks and hollows was studied (table 2.2). The patterns did not change throughout a model run. Pattern StringReal, StringOrient, MazeReal, MazeOrient and DottedReal were obtained from ArcMap by first applying a maximum likelihood classification to an aerial photograph in order to differentiate between hummocks and hollows. After this the pattern was overlayed with the domain parallel or perpendicular to the flow direction and clipped out. By using the programme Engauge digitizer the coordinates of the polygons were extracted. Engauge digitizer can load images and set reference coordinates after which the points along hummocks or hollows can be inserted by hand. These points were exported after which they were implemented in R as individual polygons in order to create the spatial discretisation. Pattern HomHum and HomHol were homogeneous, so did not need any pattern extraction or alteration. Pattern StringBufHum and StringBufHol were created in R by placing buffers of 1 meter (resulting in a 2 meter enlargement of a microform) around the hummocks or hollows of pattern StringReal.

From the calibration runs (see section 2.4.4) the best parameter set was selected to perform the scenario runs on. For each scenario and each time step the average groundwater level, the in- and out- going flux over the boundary and the evapotranspiration were saved. By comparing scenario StringReal and StringOrient, and scenario MazeReal and MazeOrient the effect of orientation was studied. Pattern StringReal and MazeReal were perpendicular to the streamline whereas StringOrient and MazeOrient were parallel. By comparing scenario StringReal, StringBufHum and StringBufHol the effect of hummock and hollow size was studied. Scenario StringReal was the original field pattern, StringBufHum has larger hummocks and StringBufHol has larger hollows. By studying pattern HomHum,HomHol,StringReal,MazeReal and DottedReal the effect of pattern type was studied.

The scenarios were compared by means of a transect of the groundwater level over the domain from south-west to north-east (figure 2.7). Another comparison was made by calculating the time needed per scenario for the average groundwater level to go back to the initial condition value, and looking at the shape of the groundwater peak over time. Furthermore the ratios of in- and out-going fluxes were studied.

Discretisation

Spatial For the model a refinement of nodes around areas of interest was used. This was done so the borders between entities (hummock and hollow) were depicted more accurately and modelled at a smaller spatial scale. By using a refinement the effect of changing hydraulic conductivity could be studied in more detail, whilst limiting the run time. The areas further away from a change in entity have a larger distance between nodes (figure 2.8 bottom). This refinement of nodes was accomplished by using finite elements. Finite differences would not be able to represent complex systems that can have a steep gradient. Finite volumes would be able to achieve this, but is mostly used in 3D situations as it is able to differ the discretisation in depth as well. With finite elements this would not be possible, but since the model is 2D this was not necessary (Bogdon, 2013).

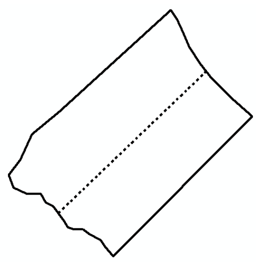

Figure 2.7: The location of the transect (dotted line) in the domain

Three methods for setting the discretisation were used. The first method was using the FVFE2D package created by Paul Torfs. In this method a formula was created with the borders of entities as input. This formula sets a node density at this border, which decreases over a certain distance which can be entered. After this distance a different node density occurs. This method works well for smaller amounts of nodes, but becomes very time extensive when used for larger amounts. The second method was using the raster to TIN tool in ArcGIS. This tool generated a triangulated irregular network from an input raster. This tool, however, did not generate the desired discretisation as many points were placed outside the domain, and some borders of entities had no nodes at all. The third method used was creating a mesh in Gmsh (Geuzaine and Remacle, 2009), which is a programme created for generating finite element grids. By using an R script the proper input for Gmsh was created, which consisted of coordinates of the border of entities which were then connected with lines. Along with this the points and lines of the domain were entered and some parameters were assigned (Avdis and Mouradian, 2012). These parameters were the node density at (LcMin) and away (LcMax) from the entity border and the distance over which this changed (see top figure 2.8). The parameters used to create the mesh shown in the bottom of figure 2.8 were a LcMin of 4 meter, a LcMax of 50 meter, a DistMin of 4 meter and a DistMax of 6 meter. This method created the desired nodes and was therefore implemented in the model.

Temporal The same principal as the spatial discretisation was used for the temporal discretisation. Around points of interest smaller time steps were taken. Since the precipitation event was at the start of the model run, and after this no further changes were made in either the model itself and in the meteorological data, this was the only point of interest. Because the flow in the model is proportional to the head differences, the lowering of the groundwater table will occur more or less exponentially. After the event, the groundwater level decreased rapidly since the hydraulic conductivity is higher closer to the surface. After a certain amount of time, the lowering of the water table proceeded less rapidly. Therefore the time step started at half an hour (interval of the meteorological data) and increased by a factor 1.2 after every time step This made sure the precipitation event and the time shortly after were modelled in detail, whereas the rest of the time the model needed less detailed steps which resulted in a shorter runtime. In order to have the variable time step the precipitation and evapotranspiration data were made cumulative.

2.4.4 Validation and calibration

Prior to the scenario runs, two validation runs were performed; one for the same time period as the model run and one for a different period. The validation runs were performed prior to the calibration runs, as the decision on which parameters were altered during the calibration, was based on the outcome of the validation of the model. During the validation runs all parameters and input values remained the same as for the scenario runs, except for the precipitation and potential evapotranspiration, for which the measured data during that period was implemented. Since the domain was selected at the location of pattern scenario StringReal, this pattern was used for the validation runs. The validation for a different time period was performed since the period for the scenario runs is quite exceptional regarding the drought and starting groundwater level. The time period was selected on the median pre rain value of the groundwater table (16.7 cm below the surface) and the average amount of precipitation during a growing season from Nijp et al. (2015). The validation run started at 27-6-2004 19:00 and ended at 29-6-2004 23:30. The time step used was half an hour for the entire run, so it could be studied in more detail.

In order to validate the model, the model run was compared with the observed values of the groundwater level by means of both the NSE (Nash-Sutcliffe efficiency) and the KGE (Kling-Gupta efficiency). A NSE of 1 means

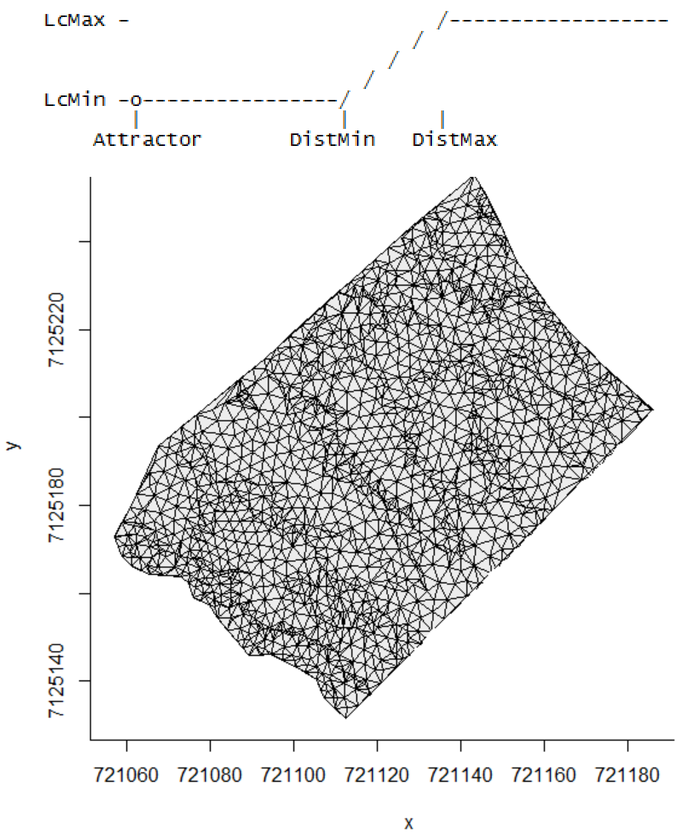

Figure 2.8: Top: description of the parameters from the Gmsh tutorial created by Geuzaine and Remacle (2009). The attractor is the line on which the refinement is based. LcMin is the node density in the same unit as the input map from the Attractor until DistMin. DistMin is the distance from which the node density starts changing until it has reached the node density assigned away from the lines of interest; LcMax. The distance over which the node density goes from LcMin to LcMax is the distance between DistMin and DistMax. Bottom: the mesh designed in Gmsh (triangle network) for pattern scenario StringBufHol, with refinements along the hummock-hollow borders

a perfect fit, a value of 0 indicates that the mean of the observed values is as good a predictor as the model and a negative value shows that the model is a worse predictor than the mean. The KGE was used since it could be subdivided into a part corresponding to the mean, standard deviation and correlation (Gupta et al., 2009). By doing this it could be observed where the model performed best, and where improvements were needed.

During the validation the water balance (flux over the boundary conditions, evapotranspiration, etc.) of each time step was studied in comparison with the NSE and KGE for the groundwater level. Through this, some parameters that could possibly improve the model by altering them were obtained. Running an elaborate parameter sensitivity was not possible due to time constraints, so a few possible sources of error were determined which were then used in the calibration runs. During the calibration these parameters were altered one by one based on the observations during the validation. This resulted in 9 calibration runs (see table 2.3) for which the NSE and KGE were calculated in order to study the effect of changing a parameter. The last calibration run was performed on a different pattern scenario than the other runs, in order to compare the evapotranspiration runs in the scenario runs where the most extreme effects of this were expected (a lot of hummocks were present). Therefore no NSE and KGE could be calculated, but the calibration run was compared with a model run without the parameter adjustment.

Which parameters were used for the scenario runs was based on the NSE and KGE with a main focus on the correlation. This was done since the observation point for groundwater was outside of the domain on an area with a different slope, so variations in the mean can be expected.

Table 2.3: The calibration runs and the reason they were performed.

Calibration run	Reason for calibration
10 % Increase gradient of the boundary conditions	Large fluxes were found over the boundary conditions, and since the conditions were an estimation the sensitivity to a 10 % increase in gradient was tested.
10 % Decrease gradient of the boundary conditions	The same reason as for the 10% increase, but now a decrease was implemented, since it was not known in which direction the boundary gradient should be altered.
Upstream boundary condition set as no-flux boundary	This was another calibration run for the boundary condition. As the incoming boundary flux was large, it was now set at 0 to study the effect of this.
50 % Decrease gradient of the downstream boundary condition	The groundwater level in the model was lower than observed (so too much outgoing fluxes) and since the slope decreases at the downstream boundary this was seen as one of the possible overestimated fluxes.
Local slope used as gradient for the boundary condition	For the model the gradient over 100 meter is used, which may not be an accurate representation. By this run the importance of local slope was tested.
Initial condition groundwater level at 16.7 cm below the surface	This run tests the effect of the initial condition on the model, as an error was expected here, since the initial condition was a very low groundwater level.
Less sharp decrease of storage over depth	The groundwater levels decrease faster than the observations, which could be caused by a too fast decreasing storage over depth.
Less sharp decrease of hydraulic conductivity over depth	The groundwater levels decrease faster than the observations, which could be caused by the hydraulic conductivity function.
Evaporation parameters of lawn used instead of hollow	The model gave lower evapotranspiration values than the observations. Lawns are still able to evaporate at lower groundwater levels than hollows, so the parameters for lawns were used.
Elevation differences between hummocks and hollows implemented	As a smoothed DEM was used, the elevation difference between hummocks and hollows was neglected which was mainly expected to effect the evapotranspiration parameter, as this was a reduction function over depth. By neglecting this difference the evapotranspiration for hummocks could be overestimated as the limiting groundwater depth was reached later. In this run (scenario 5ET) the reduction function was adapted for hummocks to have a 0.3 meter higher elevation than hollows.

3 | Results

This section will show the results obtained with the previously explained methods. The same set up as for the methods is used: first the results from the fieldwork and the analysis are presented, then the results from the model study are presented. The metadata from the field measurements is presented in appendix C.

3.1 Porosity

The particle density was found to be normally distributed for both hummocks and hollows and for each depth. The Shapiro-Wilk test showed significance values ranging between 0.107 - 0.891 meaning that the hypothesis of normality cannot be rejected. Therefore the two tailed t-test could be performed, which showed that hummocks and hollows do not differ significantly in porosity with a F-value of 0.001, 9 degrees of freedom and a p value of 0.792. The Pearson correlation to test the dependence on depth resulted in a ρ of -0.543 with a significance of 0.009. This means that the porosity significantly declines over depth (see appendix D). The fitted parameters led to the following porosity function: $\rho = (94.75611 + D * -8.147998)/100$ (D is the depth in meters below the water table) with a RMSE of 0.04 and an R^2 of 0.295 (see appendix D).

3.2 Hydraulic conductivity

The hydraulic conductivity was calculated as a function over depth for hummocks and hollows separately. First the hydraulic conductivity was averaged for each depth. This led to the values in table 3.1. It can be seen that hollows have a higher hydraulic conductivity closer to the surface. At a depth of 150 cm the hydraulic conductivity for hummocks and hollows is the same. The standard deviations are quite high (often higher than the average hydraulic conductivity), especially close to the surface. There were more measurements taken at the surface (table 1) which explains some of the declining standard deviation over depth.

Table 3.1: The average hydraulic conductivity and standard deviation for each depth relative to the water table, at hummocks and hollows.

Hummock depths [cm]	K [m/d]	Std dev [m/d]	Hollow depths [cm]	K [m/d]	Std dev [m/d]
10-20	2.984	7.85	10-20	19.066	13.42
30-40	0.236	0.32	30-40	2.920	4.40
60-70	0.037	0.07	60-70	0.873	1.63
100-110	0.003	0.003	100-110	0.016	0.02
150-160	0.004	-	150-160	0.004	0.00

The fitted parameters a and b(table 3.2) were significant for both hummocks and hollows (P values from 0.0036 till 0.0098), the c values were insignificant with a p value of 0.22 for hollows and a p value of 0.32 for hummocks. The RMSE of the fitted function for both hummocks and hollows are quite low, with hummocks having the best fit (see table 3.2). This can also be seen in the plot of these functions with their 5 % and 95% interval (figure 3.1). The intervals of the hummock are closer to the fitted function than for the hollow. It can be seen that there is overlap between the confidence intervals of hummocks and hollows from a depth of 90 cm below the water table. Closer to the surface there is no overlap.

Table 3.2: The found parameters (a,b and c) and the RMSE for the fitted hydraulic conductivity function for hummocks and hollows.

Pattern entity	a	b	c	RMSE
Hummock	20.65	0.13	0.013	0.05
Hollow	40.72	0.05	0	0.36

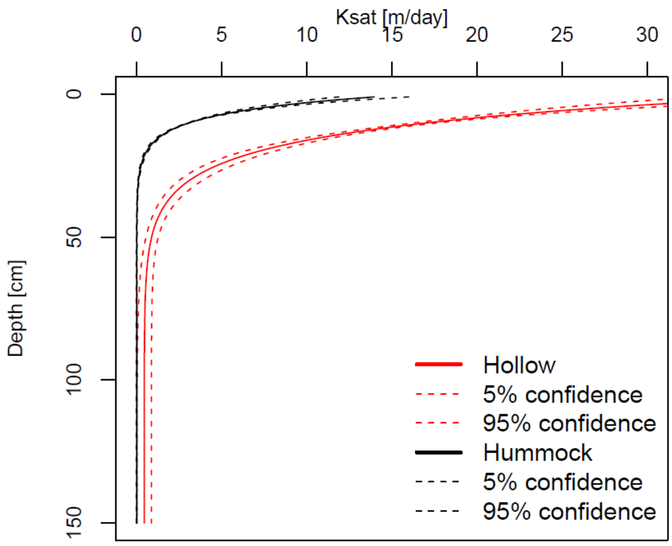

Figure 3.1: The fitted functions for hummocks and hollows with their 5 % and 95% confidence bands

3.3 Reference measurements

The reference measurements had quite some variation in their hydraulic conductivity. The average for the hummock was 9.93 m/d with a standard deviation of 2.29 m/d. The hollow had an average of 0.77 m/d with a standard deviation of 1.07 m/d. To test whether this variation was due to swelling and shrinking of the peat due to groundwater level changes, a Pearson correlation was used(table 3.3).

Table 3.3: The results from the Pearson Correlation between the hydraulic conductivity for hummocks and hollows and the groundwater level.

Pattern entity	Pearson Correlation (%)	Significance (2-tailed) (%)
Hummock	-0.120	0.880
Hollow	-0.265	0.667

From this it becomes apparent that the hydraulic conductivity is not significantly correlated to the groundwater level. Therefore no groundwater correction was performed on the hydraulic conductivity measurements.

3.4 Evapotranspiration

For the method used by Jackson et al. (1977) a site specific parameter (B) was calculated on the reference site on a cloudless day. Only one infra red photo was taken of this site on a sunny day, resulting in a value of B of 0.22. The resulting evapotranspiration values ranged between 0.646 (sunny conditions) and 0.003 (cloudy conditions) mm per hour. The data was found to be normally distributed for both hummocks and hollows. By using a paired t-test the observed (eddy covariance) evapotranspiration was compared to the calculated (infra red) one. The average calculated evapotranspiration is 0.32 mm per hour, whereas the observed value is 0.11 mm per hour. The paired t-test showed a significant difference between the observed and the calculated evapotranspiration with a $p < 0.001$. This means that the infra red method cannot accurately calculate the evapotranspiration. This was already mentioned by Seguin et al. (1982), who stated this method could be used to study spatial variations. A paired t-test was also used for comparing hummocks and hollows. As can be seen from figure 3.2 there is only a small difference between hummocks and hollows with hollows having a slightly higher evapotranspiration value. This also becomes apparent from the average, which is 0.34 mm per hour for hollows and 0.32 for hummocks. The paired t test showed this difference to be significant with a significance value of 0.001. Therefore hollows have a higher evapotranspiration than hummocks. Since this difference is counter intuitive and an possible explanation for this difference was found (the higher groundwater level of hollows might have had an effect resulting in lower temperatures), the same evapotranspiration is used for hummocks and hollows in the model for shallow groundwater levels.

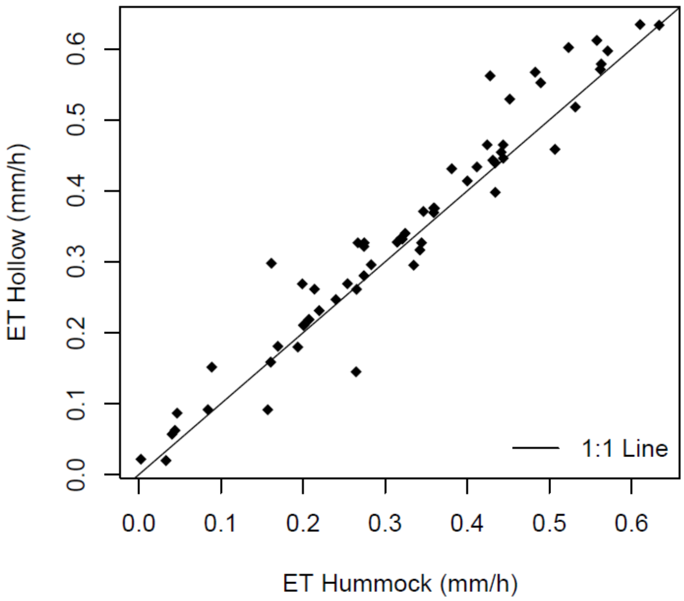

Figure 3.2: The evapotranspiration (ET) pairs of hummocks and hollows plotted against each other with a 1:1 line

3.5 Model validation and calibration

The validation of the model showed a poor fit; the NSE of the validation during the different period as the scenario runs was -2.89. The KGE is slightly better at -0.106. The correlation value was -0.1 (a good value is close to 1), the mean coefficient was 0.014 and the standard deviation coefficient was -0.097 (good values are close to 0). This means that the model does predict the mean and its standard deviation well, but does not produce a realistic groundwater level trend. The results of the validation run for the same time period as the scenario runs can be seen in the top row of table 3.4. For this validation run the correlation run is good, but the mean and standard deviation result in a low KGE and NSE. The calibration runs can also be seen in table 3.4. The calibration run where the outgoing boundary gradient is reduced by 50% shows the best KGE, but also has the lowest correlation value. The calibration run that performed the worst is the run with a incoming boundary flux of 0. There is no model run which is much better than the original on all aspects, therefore the original run was used for the pattern scenarios.

Table 3.4: The coefficients, KGE and NSE for the calibration runs and for the validation run during the same run period as the scenario model.

Calibration run	Correlation coef.	Mean coef.	Std dev coef.	KGE	NSE
Original	0.968	0.320	3.377	-2.392	-14.434
Boundary in zero	0.967	0.417	4.149	-3.170	-22.928
ET lawn	0.967	0.346	3.353	-2.371	-14.912
Boundary gradient plus 10 %	0.968	0.293	3.263	-2.277	-13.063
Boundary gradient min 10%	0.969	0.352	3.503	-2.520	-16.104
Initial condiction 16.7	0.957	0.162	3.988	-2.992	-16.295
Boundary condition local slope	0.965	0.300	3.445	-2.458	-14.480
Boundary min 50% out	0.189	0.026	0.289	0.139	-16.718
Hydraulic conductivity	0.969	0.483	3.947	-2.976	-23.444
Storage	0.892	0.133	3.648	-2.652	-15.977

The model run 5ET did not show better results than the others. The evapotranspiration was lower as the original scenario StringBufHum run. It was reduced earlier in hummocks due to the elevation difference. The groundwater level however, decreased faster than for scenario StringBufHum.

3.6 Pattern scenario runs

The patterns generated in R and ArcMap can be seen in figure 3.3. The patterns resulted in various peak responses. The effect of the pattern on the model can be clearly seen in figure 3.4. This figure shows a transect over the length of the domain from south-west to north-east after 1.5 days, as depicted in figure 2.7. Scenario StringOrient has more hollows at the start of the transect resulting in a steeper hydraulic gradient, which decreases after more hollows are present. The groundwater level rises above the peat surface at the end of the catchment. At scenario StringBufHum the accumulation of water before hummocks can be seen; the water is retained in a hollow, when a hummock is reached the groundwater level drops more quickly. At this scenario the groundwater level is more variable and less smooth over the transect. The pattern type can thus have a substantial effect on groundwater behaviour.

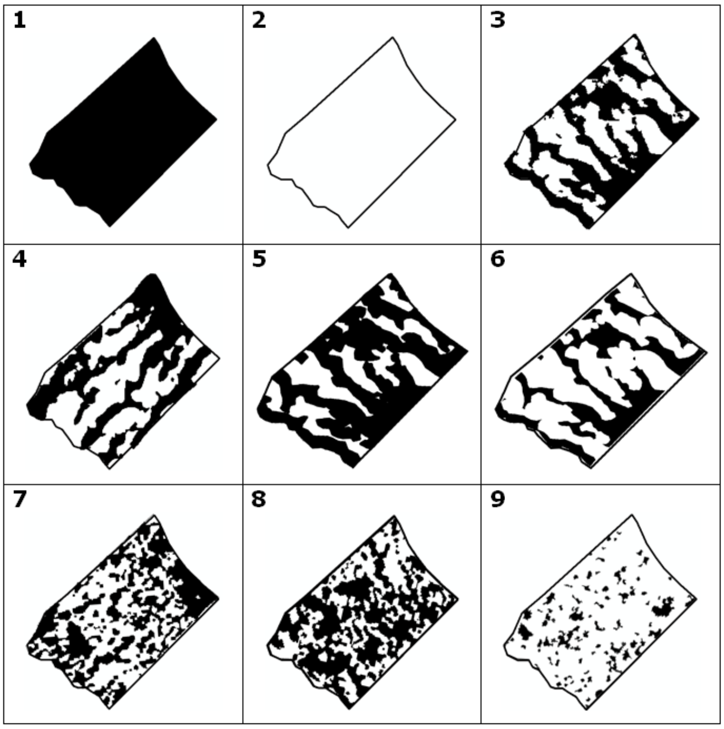

Figure 3.3: The extracted and generated patterns used as scenarios for the model runs. Hummocks are depicted black and hollows white

These differences between scenarios can also be seen when looking at the time needed for the groundwater level to return to the initial state, after the precipitation event (table 3.5). Scenario StringBufHum dries out the fastest whereas scenario DottedReal has the longest return time. The progression of the groundwater level over time can be seen in figure 3.5.

Table 3.5: The time for each scenario to go back to the initial condition prior to the precipitation event.

Scenario	1	2	3	4	5	6	7	8	9
Return time [days]	4.3	3.3	2.6	9.9	1.5	11.9	8	12.1	13.2

Pattern DottedReal takes the longest time to return back to the groundwater level before the precipitation peak (figure 3.5). When looking at the entire time period, scenario StringBufHol dries out the slowest. Scenario HomHum and HomHol show the difference in hydraulic conductivity between hummocks and hollows; scenario HomHol dries out faster since hollows have a higher hydraulic conductivity. When comparing scenario StringReal with scenario StringOrient, and scenario MazeReal with scenario MazeOrient, it becomes apparent that a pattern parallel to the

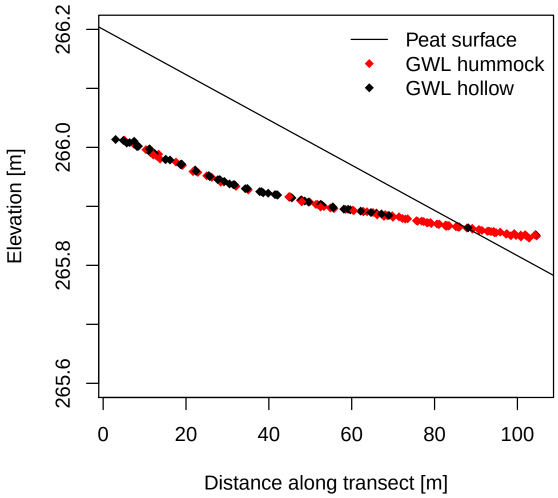

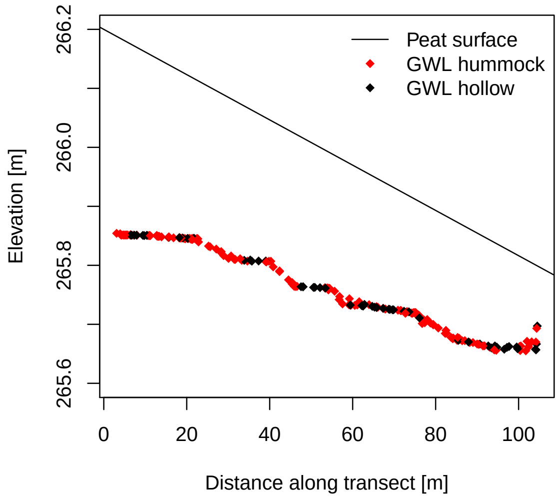

Figure 3.4: Transect of scenario StringOrient (left) and StringBufHum (right) after 1.5 days. Depicted is the groundwater level (GWL) relative to the peat surface. The difference in the groundwater level progression is due to the different pattern scenario

stream direction dries out less fast that a pattern which is perpendicular to the stream direction. By comparing scenario StringReal, StringBufHum and StringBufHol the importance of distance between hummocks can be seen. A larger distance between hummocks results in slower decline of the water level than a shorter distance. The original pattern lies in between the two. When comparing the various pattern types it becomes apparent that a dotted pattern can retain water the longest, after this comes the maze pattern, followed by homogeneous hummock, then the string pattern and finally the homogeneous hollow. From the figure it can also be seen that not every scenario follows the same curve; scenario StringBufHum shows an exponential decrease in groundwater level, whereas pattern DottedReal shows more bumpy behaviour. This behaviour, and the difference between scenarios can be explained by comparing boundary fluxes (figure 3.6).

Figure 3.6 shows the contribution of each in and outgoing flux to the total in and outgoing flux. From scenario HomHum it can be seen that the incoming and outgoing flux are balanced (around the 0.5 line). As the groundwater level decreases over time, both evapotranspiration and outgoing boundary flux are reduced. The evapotranspiration is reduced through the implemented reduction function in the model. The boundary fluxes decrease as the hydraulic conductivity becomes lower at lower groundwater levels. It can be seen that the evapotranspiration reduces faster, as the fractions begin to shift. Thus the hydrological feedback of evapotranspiration is stronger than the decrease of water loss through conductivity. The distribution of the incoming fluxes are the same for each scenario, as the precipitation flux is fixed, so after the precipitation event the incoming fraction becomes 0, which makes the incoming boundary flux have a fraction of 1. The incoming boundary flux can be studied trough the BCout/BCtotal line. Scenario StringBufHum has a higher outgoing boundary flux than ingoing, which is possibly caused by the lack of hollows at the incoming boundary. This explains the fast decline in groundwater level (see figure 3.5). As already explained for scenario HomHum, both the evapotranspiration and boundary fluxes decrease as the groundwater level drops. Since the groundwater level drops the most at this scenario, a shift in fractions between the boundary flux and evapotranspiration can be seen. After approximately 22 days, the evapotranspiration becomes lower than the outgoing boundary flux. When comparing scenario HomHum and StringBufHum to scenario StringBufHol and MazeOrient, the reason for the bumpy line in figure 3.5 can be found. Scenario HomHum and StringBufHum show a more or less constant ratio between in and out coming boundary fluxes, whereas for scenario StringBufHol and MazeOrient this division is more variable. As it changes how much water goes in and out, the groundwater level responds accordingly, creating the more bumpy line. From scenario StringBufHol it can be seen that the incoming boundary flux is always larger than the outgoing flux, which explains why this scenario dries up the slowest. The fraction of evapotranspiration starts out lower, meaning that there is quite some outgoing boundary flux. The same

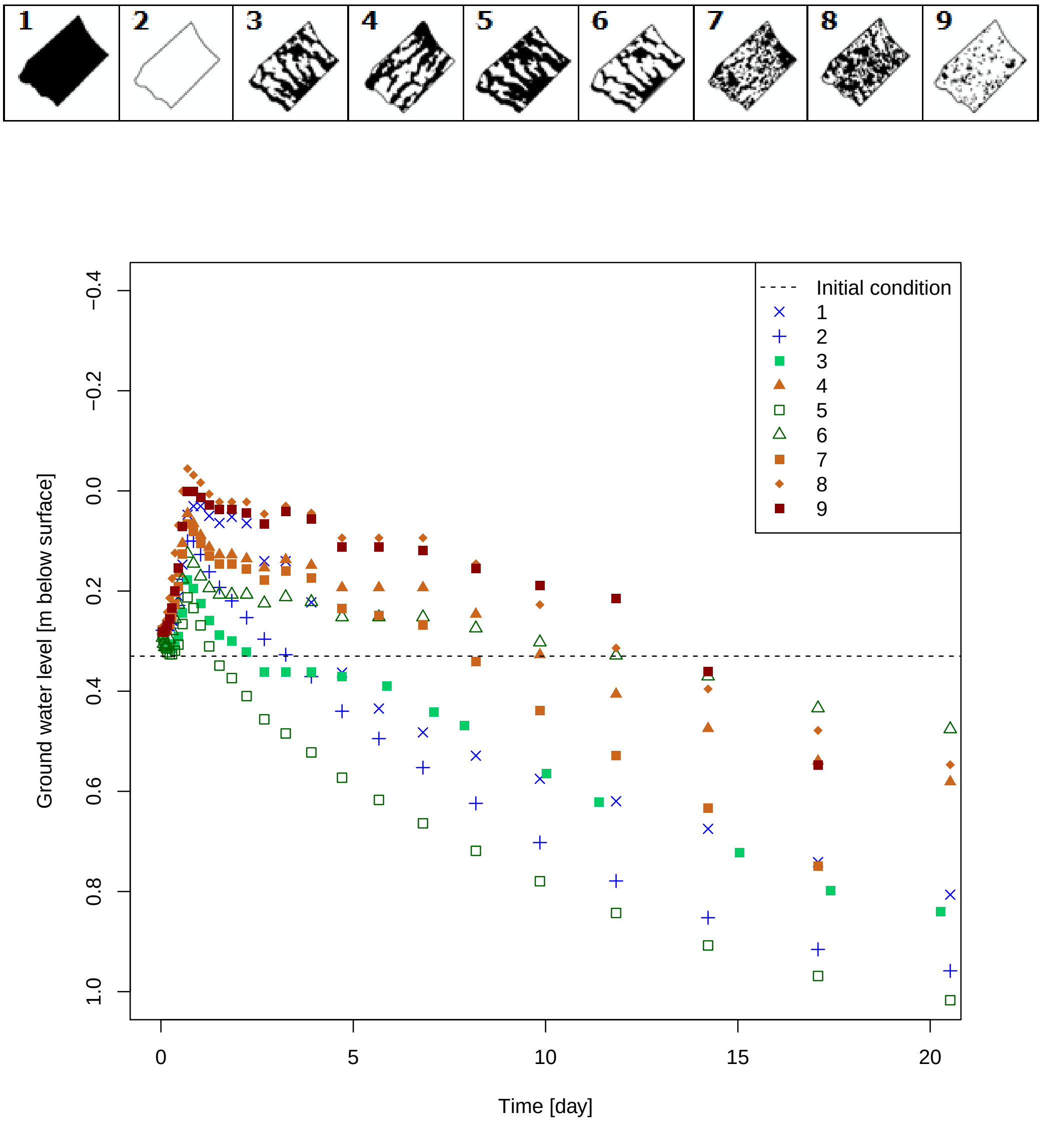

Figure 3.5: The average groundwater levels over time for each pattern scenario. The dotted line is the groundwater level at the start of the model run

can be seen for scenario MazeOrient, though scenario StringBufHol displays this in a more extreme measure. Both do not show a shift in evapotranspiration and the BCout yet, as the groundwater level has not dropped far enough yet for the evapotranspiration to be strongly reduced.

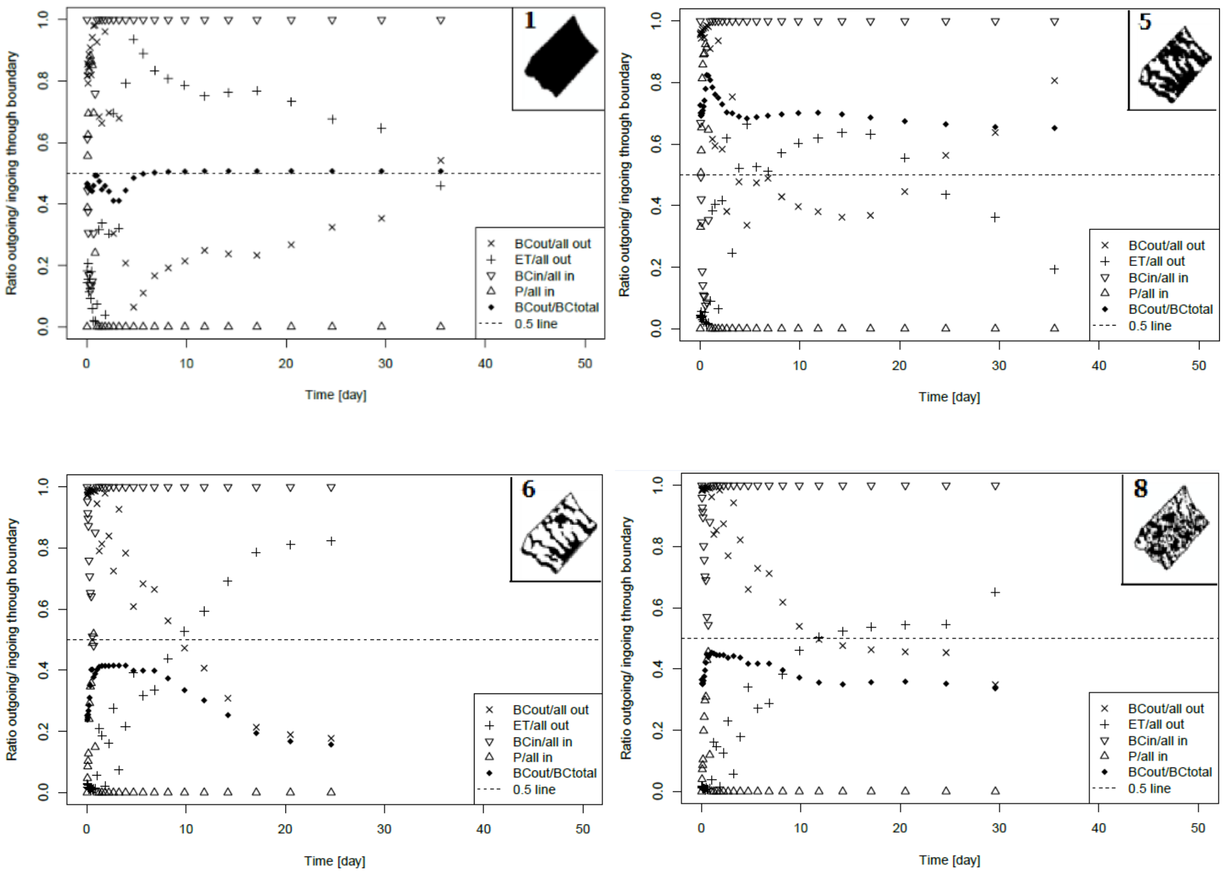

Figure 3.6: Time series of ratios of in and outgoing fluxes for scenarios HomHum (top left), StringBufHum (top right), StringBufHol (bottom left) and MazeOrient (bottom right). The outgoing fluxes (ET: evapotranspiration, BC: boundary condition flux) are divided by the total outgoing amount in order to get the relative contribution. The same is done for incoming fluxes (P: precipitation, BC: boundary condition flux). In order to compare the in and out going boundary fluxes the BCout is divided by the total boundary flux. The fraction of BCin is then 1 minus BCout/BCtotal

4 | Discussion

This chapter provides a discussion of uncertainties and the results with possible explanations for some observed phenomena. First the fieldwork and data analysis are discussed. Second the model runs and output are discussed.

4.1 Fieldwork and data analysis

4.1.1 Hydraulic conductivity

The hydraulic conductivity measurements were shown to be prone to errors; a large unexplained variability can be seen in the reference measurements. This means that the measured conductivity values are often over or under estimated. This error is not likely to be caused by disturbance through piezometer installation, but by inaccuracy of the method; the reference measurement is only installed once and maintains a large deviation in hydraulic conductivity values over the field period. The reason for this could be variations in water addition as some inaccuracy from this is expected. However, this variation is not expected to be as large as the variation found in the measurements. Another explanation for the variation is by the fitting method used in R. End points were often determined by hand, causing differences in the time selection between measurements. This could have influenced the outcome, leading to variation. Other possible explanations for variation at all other measurements could be different degrees of clogging of the piezometer filter, installation disturbances, unaccounted for groundwater level variations, wrongly used time intervals and diver errors. These errors could have resulted in a different hydraulic conductivity, or a missing value since no calculations could be performed. Another possibility is the spatial variation of hydraulic conductivity, which was not studied here. Differences can be expected in hydraulic conductivity between various microform sizes as smaller microforms might have less strong feedbacks and may thus have been a different microform in the past, which would lead to a different hydraulic conductivity profile over depth. Differences can also be caused by the place in the landscape and the local landscape; the landscape can result in differences in the peat formation and thus possibly in the hydraulic conductivity. However, as the reference measurements already showed a large variation, a large part of the variation is expected to be due to errors in the measurement and the calculation.

Furthermore the method used to calculate the hydraulic conductivity directly after piezometer installation might have led to more errors. During piezometer installation the pressure differences in and outside the piezometer are large. Baird et al. (2004) and Hvorslev (1951) advised to use small pressure differences to prevent errors. Also errors could be caused by the measurement being close to piezometer installation. The surrounding peat has not had time recovered yet, so it can be either be compressed by pushing the tube in, or there may be a gap around the piezometer caused by the pre drilling with the gouge. Possibly water flowed in when pushing the piezometer downward as the filter passed layers with higher conductivities. Nonetheless it was decided to use these measurements, as the calculated values were in the same order of magnitude as measurements calculated with the slug test and to expand the dataset; this method was mostly used at larger depths (100 cm) and only few hydraulic conductivity values were obtained at this depth. The found values were also in the same order of magnitude as found by Baird et al. (2015) at 90 cm depth.

Previous to the hydraulic conductivity calculation, the measured pressure was accounted for groundwater level changes. However, only changes due to precipitation and evapotranspiration were taken into account and groundwater flow was neglected. This flow is not expected to have a very large impact on the short time scales (slug tests of a few minutes or hours), but for the measurements at larger depth (duration of multiple days) this might have had an impact, especially when after a precipitation event a peak passes. The precipitation, evapotranspiration and porosity were assumed equal over the entire mire, which can also lead to wrong corrections. This might be the cause of some of the measurements where no hydraulic conductivity could be calculated. Some measurements showed fluctuating pressure levels that were not filtered during the correction. This could also be caused by defect divers, as some showed patterns which were unrealistic for groundwater fluctuations. For future studies, an additional piezometer could be placed close by the hydraulic conductivity measurement (but not so close it influences the measurement) that continuously monitors the groundwater level. By doing this it can be assured that the data correction is correct.

Not all depths of the original sampling scheme were reached due to higher stabilization times than expected. As most of the variation in hydraulic conductivity occurs near the peat surface, this does not have a large effect on the fitted hydraulic conductivity function over depth. Due to the longer stabilization times, more sites were selected where only the first two depths were measured. This was done both to get more measurements and to get a better coverage over the mire. It was not part of this study, but it would be interesting to study the locations effect on the hydraulic conductivity. For example the distance to the outlet could be of importance, as close to the outlet relatively more water flows through the soil, which could have an impact on vegetation or decomposition of the peat.

Despite all the possible errors described above, a clear difference in hydraulic conductivity between hummocks and hollows was found (table 3.1) in accordance with Loisel and Yu (2013); Rydin et al. (2013); Yuan et al. (2015). Baird et al. (2015) and Branham and Strack (2014) did not find a relationship of hydraulic conductivity over depth. Holden and Burt (2003) found a relationship over depth at some sites, but there were also sites where no relationship of hydraulic conductivity over depth were found. In this study a strong relationship to depth was found, which is in accordance with the findings of Branham and Strack (2014); Boelter (1965); Clymo (2004); Päivänen et al. (1973); Rydin et al. (2013); van der Schaaf (1999), who explain this through the greater compaction and humification of deeper peat. Closer to the peat surface, hollows have a higher hydraulic conductivity. At a depth of 90 cm and lower below the peat surface, no difference between hummocks and hollows occurs, a phenomena also found by Baird et al. (2015); Branham and Strack (2014); Kaplan et al. (2012). This means that most groundwater flow occurs close to the surface (higher hydraulic conductivity), where the difference between hummocks and hollows is the largest. Therefore hummock-hollow patterns will have an effect on the groundwater flow and thus affect peatland water retention.

4.1.2 Evapotranspiration

In the field it was difficult to take the infra red photo's under the same meteorological conditions. It was often partly clouded, or the day started cloudless but ended with thunderstorms. On a sunny day all sites were measured, but spread over the entire day as the travel times could be long and other measurements needed to be conducted simultaneously. This may have caused inaccuracies in the data analysis. As Seguin et al. (1982) already mentioned, the infra red measurements could not accurately predict the evapotranspiration. It is a good method for detecting spatial variability in evapotranspiration. In order to do this in an accurate manner, the meteorological conditions needed to be equal. By using a paired t-test this was accounted for, but it would be better to have all measurements under the same conditions. Ideally infra red time lap cameras would have been installed. In this way the surface temperature is measures simultaneously and continuously at multiple sites, so measurements from the exact same time, and thus conditions, can be compared.

The results showed a significant difference between hummocks and hollows, with hollows having a higher evapotranspiration. This is in contrast with the hypothesis, since hummocks are hypothesized to have more vascular plants that are able to actively take up water and evaporate more (Eppinga et al., 2009a,b). In the field there were also vascular plants found on hollows (a fraction of 8 per m2 less than hummocks, but different vascular plant species), that could have resulted in more evapotranspiration, as the groundwater level is closer to the surface at hollows due to the lower elevation than hummocks. As the evapotranspiration was calculated based on temperature, the higher groundwater level of hollows might have lowered temperatures (specific heat capacity difference with air is a factor of 4.23) leading to the higher evapotranspiration values. Considering the small variation between hummocks and hollows (0.02 mm per hour) and this possible effect, it was decided to assume there is no difference in evapotranspiration between hummocks and hollows for the model study (at high groundwater levels).

4.2 Model

4.2.1 Parametrization

The porosity and hydraulic conductivity were implemented as functions based on the field measurements. No large errors are expected here, though measurement errors could have occurred as explained above. The evapotranspiration was build as a reduction function, based on literature. All parameters were taken from the paper Heijmans et al. (2008). In reality the evapotranspiration will not be a linear reduction function but show exponential behaviour. During the validation of the model it became apparent that the calculated evapotranspiration was smaller than the observed value. When looking at figure 3.6 it can be seen that the evapotranspiration is the relatively largest outgoing flux, which is in line with van der Schaaf (1999) who found evapotranspiration to be the most important loss term of most Irish midland raised bogs. The model could be improved by adding more realistic evapotranspiration, either by measurements during droughts for hummocks and hollows so a groundwater reduction function can be created. Another option is to perform a more elaborate parameter calibration where various evaporation parameters are validated.

4.2.2 Technical aspects

Building the model was time extensive due to its complexity. Most time was spend on solving instabilities and smoothing functions. As the catchment model had more variability in its geology, more time was needed for this. As this time was not anticipated for in the study planning, it was decided not to use the catchment model. For the scenario model, time was still needed to solve for errors and to introduce smoothed functions. This resulted in less available time for, for example, calibration runs or more scenario runs. Though the modelling situation was not ideal regarding the time aspect, the used package and modelling environment were suitable for this study. Another environment could have been used (e.g. Modflow), but as the model is complex this would have led to various difficulties as well. At this point, more suitable models for this kind of problem are not available. Therefore improving the catchment and scenario models for further studies would be more efficient than starting over with a different method or model environment.

4.2.3 Set up

In the set up various possible sources of error were present. Since the catchment model could not be used, the initial and boundary condition were estimated. The initial condition was set equally over the entire domain, using a groundwater level value approximately 200 meters outside of the domain. The groundwater level in reality will not be the same for the entire domain, and the value will be different since the used measurement was not taken inside the domain but at a location nearby, with a different slope. This might have had an effect on the results and have effected the differences between scenario's and their in and out going fluxes. How big this effect was, is not known as there were multiple possible sources of error. In order to find out, a sensitivity analysis on the initial condition could be conducted. It would be better to have groundwater measurements at various locations inside the domain itself, or to use a catchment model to simulate these values. Another option as mentioned by Franke et al. (1987) is to first perform a steady state simulation, of which the outcome can be used as initial condition for the transient model. This would be a good option as it does not require additional groundwater level measurements or large changes to the model, and is less time intensive than an elaborate sensitivity analysis. By running the model for a period of time (required period not yet known), before applying the precipitation event and drought, possible errors in the initial condition have had the time to level out, and spatial variation in the groundwater level will be present in the model.

Another error is expected because of the boundary condition. A fixed gradient parallel to the surface elevation is imposed. The flux varies through the difference in hydraulic conductivity over depth and between hummocks and hollows. Haitjema and Mitchell-Bruker (2005) found that in wetlands the groundwater table follows the topography, so the fixed gradient is a good approximation. However, Haitjema and Mitchell-Bruker (2005) also found that the local slope does not influence the local gradient of the groundwater. As the domain is quite small, the fixed gradient may be incorrect. This also becomes apparent when looking at figure 3.4 which shows that the groundwater gradient in the model is not parallel to the surface gradient. Furthermore a change in gradient could be expected over time, as an extreme precipitation event is followed by an extreme drought. The boundary flux reacts very strongly to the fast decreasing hydraulic conductivity and to the microform type. This results in a high variation between the different scenarios, which may not be correct. It might be better to put a fixed flux, preferably based on measurements, as incoming boundary condition and only have the outgoing boundary flux as a Cauchy boundary. This would limit the errors of the incoming flux. Setting the outgoing flux as fixed would not be an option, since then the effect of the pattern cannot be studied any more. Another option would be to not set a boundary condition at the outgoing boundary. The effect this would have was not studied here.

As open water flow was not modelled, the water above the peat surface was immediately removed. However, as can be seen in figure 3.4 the groundwater level did reach values above the surface. This is caused by the more rapid flow through the hollows, which causes accumulation when a hummock is reached. As a fixed gradient is put at the boundary condition, the water may not be able to flow out of the domain fast enough, causing this phenomena. What cannot be explained directly is why this excess water was not removed by the function implemented to do so. This could either be a model error, or it has to do with the order in which the functions work; the water above the surface could be removed prior to the groundwater flux calculation, which causes the water to rise above the surface again. The exact cause was not found in this study, but this should be fixed or open water flow should be included when improving the model. The high water table did not lead to model errors; when the hydraulic head reached values higher than 0.5 cm below the surface, the hydraulic conductivity was set to the value at 0.5 cm below the surface. This was done to prevent unrealistically high values, or errors when the water table would reach values above the surface.

Another possible error is due to the smoothed DEM. This was necessary so the elevation differences caused by the original pattern inside the domain would not affect the various pattern scenarios. By doing this, however, the evapotranspiration of hummocks is overestimated as the limit is reached later since the elevation of hummocks is lowered, resulting in shallower water levels and prolonged evapotranspiration during drought. Therefore the differences between hummocks and hollows could be underestimated. By implementing an adjusted DEM based on the pattern scenario this could be prevented.

The chosen patterns were selected to be as realistic as possible. For the realism of the model run this is a good asset. For the prediction of the pattern that holds water the best, however, it is not. At this point it is not know whether the change in return time is due to the pattern type or the fraction of hummock and hollows. The true effect of the patterns can be tested by using various patterns, orientations and microform size, whilst maintaining the same ratio between hummock and hollow area. This could be done by creating the patterns through multiple-point geostatistics, which uses training images to create accurate patterns but more control could be exerted on the ratios and the anisotropy of the patterns(Arpat, 2005).

4.2.4 Validation and calibration

The validation showed that the model is a poor predictor for the groundwater level in the area. A precise validation was however not possible, as only one groundwater measurement location was present in the mire, which was outside of the domain. This location was still nearby the domain, but had a slightly different slope and could thus behave slightly different. Because of this, less attention was paid to the exact groundwater level value and more to the correlation. As can be seen in table 3.4 the correlation was quite high (0.968). Therefore it was assumed that though the model cannot predict the right values, it can provide information on the behaviour of the various patterns. As can be seen in figure 4.1 there is no systematic bias between the observations and the model predictions. This shows that though the correlation value is high, the model is not a good predictor. Assumed here is that the error(s) which cause this are the same for each scenario run, resulting in the possibility of comparing them.

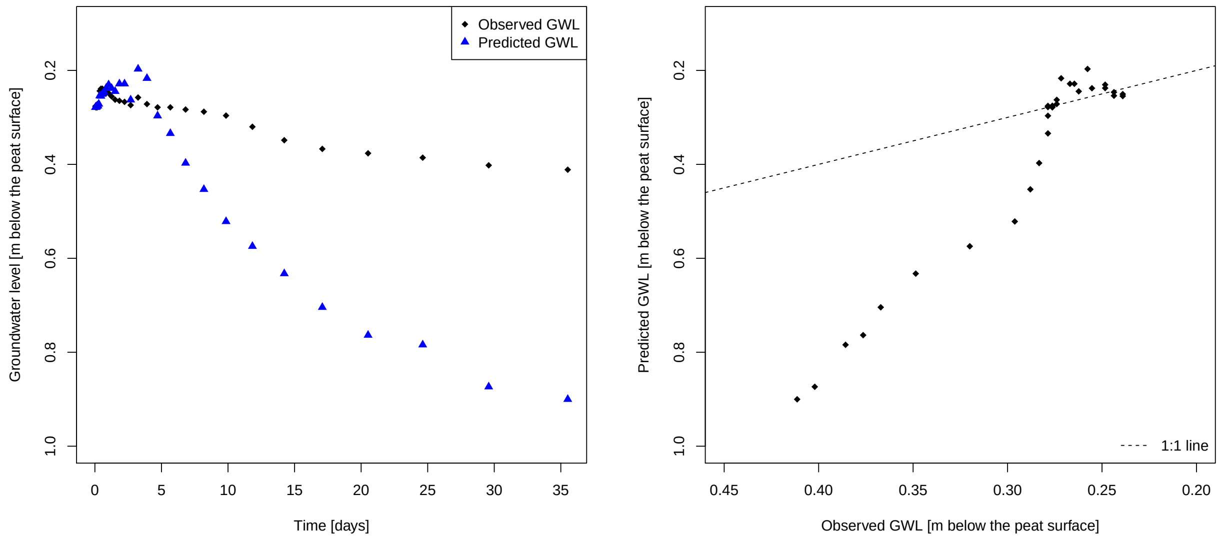

Figure 4.1: Left: the groundwater level observations and model predictions over time. Right: the groundwater level observations compared to the predictions

The calibration runs were performed based on reason; an error was expected in the boundary condition, so various calibration runs were performed on this. The reason for this approach was the time constraint. By doing this, possible sources of error could be overlooked. All calibration runs showed poor results, whereas a different parameter value, or a combination of calibration runs could have improved the model. For example the run with a strong reduction in outgoing boundary flux showed the highest KGE but a weak correlation, and was therefore rejected. By doing a more elaborate study on the calibration, the model could be improved and possibly be able to give predictions with a smaller uncertainty.

4.2.5 Pattern scenario runs

The results of this study suggest that the pattern scenario has a strong effect on the groundwater level (figure 3.4). For scenario StringBufHum the effect of blockage by hummocks can clearly be seen, which causes water retention in hollows. This phenomena was already mentioned by Baird et al. (2015); Eppinga et al. (2009b); Loisel and Yu (2013) as a feedback to maintain and amplify the contrast between patterns. By retaining the water the hollows remain wet enough, and the hummocks remain dryer. The difference consists out of a few (approximately 4) cm. Scenario StringBufHum returns to the original groundwater level the fastest (1.5 days) and scenario DottedReal the slowest (13.2 days). These drying out times should not be taken exact; as already explained above the model showed to be a poor predictor, but comparisons could be made. This means that scenario StringBufHum still dries out the fastest, and DottedReal the slowest but at which rate is still unknown. The groundwater level in scenario HomHum and HomHol behave as expected; scenario HomHol dries out faster since it has a higher hydraulic conductivity. All of the other outcomes are however unexpected. Patterns positioned parallel to the stream direction dry out slower than the ones perpendicular. It was expected to be the other way around, as the perpendicular pattern would result in more blockages. A possible explanation could be the large hummock at the outgoing boundary of scenario StringOrient in combination with the hollows at the incoming side. Scenario StringReal has a hummock at the incoming side and more hollows at the outgoing one. As it was found that the boundary conditions have a large impact, this could cause relatively more in or out flux which could explain the unexpected difference between the scenarios. When looking at figure 4.2 this theory could be supported. Scenario StringOrient shows a smaller BCout/BCtotal ratio, which means that the incoming boundary flux is relatively larger than the outgoing boundary flux. This could be explained by the hollow at the incoming boundary side, and the hummock at the outgoing side. This theory however, does not work for scenario MazeReal and MazeOrient. These scenarios also have this effect, but the other way around. Pattern MazeReal (perpendicular) has more hummocks at the outgoing side and shows a smaller ratio. It is however still found that the parallel pattern (scenario MazeOrient) dries out slower. Therefore the found effect cannot be referred to as only a boundary condition effect. An explanation for the counter intuitive find is not yet found.

From the comparison between scenario StringReal, StringBufHum and StringBufHol it is found that larger hollows results in a slower decline of the water table. The hypothesis was that this would be the case for larger hummocks, as in this pattern (scenario StringBufHum) there are relatively more hummocks which have a lower hydraulic conductivity. It became apparent that not the fraction of hummock and hollow, but the distance between hummocks has an effect on the drying out of the domain. It was found that a larger distance between hummocks results in slower drying. Possibly the hydraulic conductivity feedbacks have an optimum where a shorter distance between hummocks results in less strong water retention in hollows. It would be interesting to perform a follow up study on the optimal distance between hummocks for water retention.

It was hypothesized that string patterns would dry up the slowest. This was not found when looking at the return time to the initial condition where the dotted pattern (scenario DottedReal) was the slowest. Shortly after however, scenario StringBufHol (string pattern) has a higher groundwater table, so the hypothesis is not rejected when looking at a longer time period. When only looking at the patterns that could be found in the field, the dotted pattern dries out the slowest, followed by the maze pattern, the homogeneous hummock, the string pattern and the homogeneous hollow. The string pattern was expected to dry up slower, but as already mentioned the distance between hummocks is very important, as a larger distance would result in a much slower decrease in groundwater level. It was not expected that the dotted pattern dried up slower than the maze, as the maze contains more hummocks and seemingly more blockages. Possibly the hummock/hollow ratio also has an effect where more hummocks do not immediately mean a slower decline, due to the feedback strengths that may decrease when there are a lot of hummocks. This effect could be studied by using the same hummock/hollow ratios for various patterns, or various ratios for the same pattern, as already described in section 4.2.3.

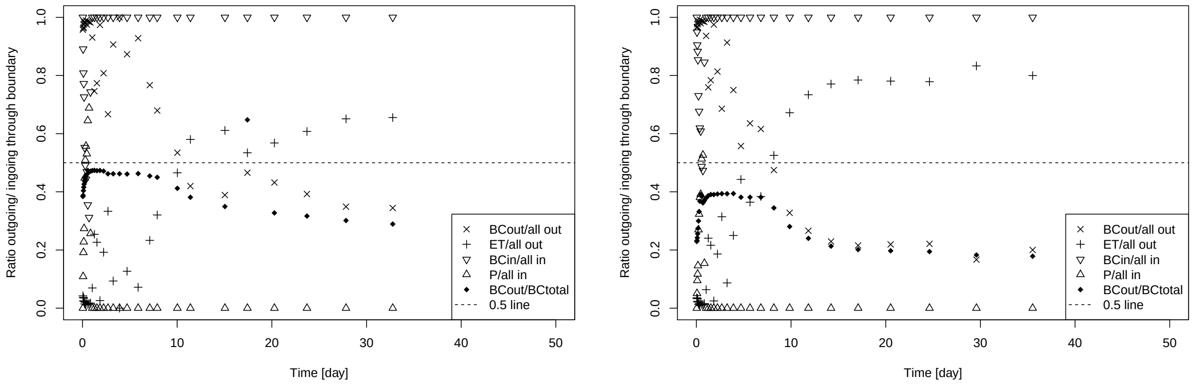

Figure 4.2: The ratios of in and outgoing fluxes for scenarios StringReal (left) and StringOrient (right). The outgoing fluxes (ET: evapotranspiration, BC: boundary condition flux) are divided by the total outgoing amount in order to get the relative contribution. The same is done for incoming fluxes (P: precipitation, BC: boundary condition flux). In order to compare the in and out going boundary fluxes the BCout is divided by the total boundary flux. The fraction of BCin is then 1 minus BCout/BCtotal

For each hypothesis only one pattern was used per scenario; e.g. only one string pattern perpendicular to the streamline was used. As there are many possibilities for a certain pattern type, the results found with the used patterns might not be true for all the patterns. If, for example, a slightly different parallel and perpendicular string pattern were used, the outcome may have shown that perpendicular strings retain water longer than parallel string patterns. As most patterns were natural (they were taken directly from the aerial photograph), no error is expected from the pattern itself. Therefore this study does show that the patterns have an impact on the hydrology of a peatland, however, the exact impact is not known as the found relationships might not be true for all patterns. It could be that the used patterns are an exception case, and by testing multiple patterns the results could be different. In order to be certain of the results found in this study, a more elaborate study is needed with multiple varying patterns within one scenario.

4.2.6 Implications for climate change impact studies on peatlands

In general it can be said that spatial organization of peatland patterns have a strong effect on peatland hydrology by increasing the retention time, as suggested by Eppinga et al. (2009b); Ridolfi et al. (2006); Rietkerk et al. (2004). A dotted hummock pattern will retain water the longest in the droughts that are expected under climate change. A string pattern with a large distance between hummocks would also retain water well. For string patterns it was found that the distance between hummocks means the difference between having the highest and lowest water retention. Therefore this parameter is seen as one of the most important ones, on which further study should be conducted.

As the peatlands in Scandinavia generally are projected to become wetter under climate change (Allen and Ingram, 2002) an increase in hollow vegetation can be expected. For the patterns this will mean that the hummocks become smaller. This change will make the area more persistent to droughts according to this study. The patterns that retain the most water (StringBufHol and DottedReal) are the ones with the most hollows (with the exception of pattern HomHol). This means that if the entire mire becomes a hollow, it will more likely become a carbon source. This is not expected to happen, since though the mire becomes wetter, there are also longer dry periods in which hummock species are favoured. Strack and Waddington (2007) found that by slightly lowering the water table, hollows show an increase in productivity and increase in vegetation leading to more carbon sequestration. Therefore climate change will not immediately lead to the peat becoming a carbon source when sufficient hollows are present, unless the water table drops below the level that results in the phenomena described by Strack and Waddington (2007). However, if the future climate is such that hummocks are favoured, the peat will dry out faster as the distance between hummocks will become smaller. This will be a positive feedback that will result in only homogeneous hummock areas which could lead to a catastrophic shift (Rietkerk et al., 2004).

The patterns have been found to have a large impact on the groundwater behaviour, and thus cannot be neglected when modelling peatlands. These patterns should be included when making predictions for peatlands under various climate scenarios The exact effect that these patterns have is not know yet, as the model used is of poor predictive quality. A next step would be to improve this model, or use a different, well preforming model and add the patterns. By doing this better predictions can be made. It would be useful to build a model that is less dependent on the now fixed boundary conditions, as this was found to have a large influence. By doing so the various patterns can be compared in a more quantitative way. It would also be interesting to combine this model with the model of Eppinga et al. (2009b) or Nungesser (2003) in which the microforms can change through time by multiple feedbacks.

5 | Conclusions

This section will give the answers to the research questions. First the subquestions are answered. Finally the main research question is answered.

Is there a difference in saturated hydraulic conductivity between hummocks and hollows?
The field study pointed out that there is a significant difference in hydraulic conductivity between hummocks and hollows until a depth of 90 cm below the peat surface. Hollows were found to have a higher hydraulic conductivity; at 10-20 cm below the water table, hummocks have an average hydraulic conductivity of 2.98 m/d, whereas hollows have an average of 19.07 m/d.

How does the saturated hydraulic conductivity change over depth?
For both hummocks and hollows the hydraulic conductivity shows a decline over depth. The functions with which they decline are as follows:

- Hummock: $k = 20.65 * e^{(-0.13*D*100)} + 0.013$
- Hollow: $k = 40.72 * e^{(-0.05*D*100)}$

Where k is the hydraulic conductivity in md^{-1} and D is the depth in m.

Is there a difference in evapotranspiration between hummocks and hollows?
There was a significant difference found in evapotranspiration between hummocks and hollows, with hollows having an average higher evapotranspiration value of 0.02 mmh^{-1}. It was decided to assume that there was no difference under non-limiting groundwater levels in the model. This decision was based on a possible error that would overestimate the evapotranspiration in hollows in combination with the small difference found and the found literature. A difference is expected at greater groundwater depths, as the vegetation on hummocks is able to evapotranspiration at potential rates for deeper groundwater tables than hollows.

How does the distance between hummocks influence the hydrology?
The model shows that a greater distance between hummocks results in a slower drying out of the peat area. The model reveals this parameter to be very important, as the test of this parameter resulted in both the most (large distance between hummocks) and least (small distance between hummocks) resilient patterns. It is found that this distance parameter is more important than the hummock/ hollow fraction in the area, as a pattern with a large hummock fraction but a small distance between them results in less water retention than less hummocks with a greater distance between them. It is suggested to perform further studies on the optimal distance between hummocks for water retention.

How does the spatial organization and orientation of hummocks and hollows influence the hydrology of a peatland?
Patterns which are parallel to the stream direction dry out the slowest. An explanation for this is not yet found. A dotted pattern is found to be the most efficient in water retention during droughts. More research is necessary to create patterns with equal hummock/hollow ratios that will provide more information on the effect of spatial organization. By testing more patterns (only 1 per pattern type is used in this study), more insight can show if the found results are always true, or are an exception.

What effect does the hummock hollow patterning have on the hydrology of a peatland?
The spatial organization of hummock and hollow patterns have a large effect on the hydrology of a peatland. The microforms can create blockages which result in a longer residence time of the water. The exact effect is not yet found due to poor model performance. The model showed a poor RMSE, but a good correlation with the observations. There is however no fixed bias found, so the model does not predict the shape and duration of water table draw downs correctly. As the same error is expected in all models, the various scenario runs could be compared. The found effects of patterns show that they cannot be neglected in further modelling of peatlands under climate change.

6 | Acknowledgements

I would like to thank everyone who has made this thesis possible. First of all my main supervisor Jelmer Nijp: thank you for providing me this interesting topic; I have learned a lot about peatlands from your expertise. Our weekly discussions were very useful, and I would like to thank you for always making time when an urgent question came up. Secondly, I would like to thank Paul Torfs: without your help I would not have had a working model. Thank you for helping me out when I got stuck and for all your great modelling advice. Thirdly, Ryan Teuling: thank you for answering my questions on evapotranspiration and helping come up with a method to measure this in the field. Fourthly, I would like to thank Arnaud Temme for answering my questions on the geology of Degerö Stormyr. I also want to thank all my supervisors for providing me with useful feedback on my thesis draft.

Furthermore,I would like to thank Edward van Westrene who conducted his study on peatlands simultaneously. Thanks to your banter and musical assistance in the field, the fieldwork was a great experience. Thank you for the mental support during the modelling and writing stage of this thesis. Finally, I would like to thank everyone from SLU (Swedish University of Agricultural Sciences) who provided materials needed in the field.

Bibliography

Alexanderson, H., Karlstom, C., and Larsson-McCann, S. (1991). Temperature and precipitation in sweden: 1961-1990. referensnormaler. Technical report, SMHI Meteorologi Report.

Allain, R. (2014). Testing the accuracy of the flir one. $url : https : //www.wired.com/2014/09/testing - accuracy - flir - one/$.

Allen, M. R. and Ingram, W. J. (2002). Constraints on future changes in climate and the hydrologic cycle. *Nature*, 419(6903):224–232.

Alterra (2013). Bepaling van het porievolume en volume van de vaste fase met behulp van de luchtpyknometer. Standaardwerkvoorschrift.

Amvrosiadi, N., Seibert, J., Grabs, T., and Bishop, K. (2016). Water storage dynamics in a till hillslope: the foundation for modeling flows and turnover times. *Hydrological Processes*.

Arpat, G. B. (2005). *Sequential simulation with patterns*. Stanford University.

Aubinet, M., Vesala, T., and Papale, D. (2012). *Eddy covariance: a practical guide to measurement and data analysis*. Springer Science & Business Media.

Avdis, A. and Mouradian, S. (2012). A gmsh tutorial. $url : http : //amcg.ese.ic.ac.uk/files/gmsh_tutorial.pdf$.

Baird, A. J., Milner, A. M., Blundell, A., Swindles, G. T., and Morris, P. J. (2015). Microform-scale variations in peatland permeability and their ecohydrological implications. *Journal of Ecology*.

Baird, A. J., Surridge, B. W., and Money, R. P. (2004). An assessment of the piezometer method for measuring the hydraulic conductivity of a cladium mariscusâĂŤphragmites australis root mat in a norfolk (uk) fen. *Hydrological Processes*, 18(2):275–291.

Barber, K. E. (1981). *Peat stratigraphy and climatic change*. Balkema.

Beers, W. v. (1983). *The Auger Hole method: A field measurement of the hydraulic conductivity of soil below the water table*. ILRI. Wageningen (Holanda).

Belyea, L. R. and Baird, A. J. (2006). Beyond "the limits to peat bog growth": cross-scale feedback in peatland development. *Ecological Monographs*, 76(3):299–322.

Bishop, K. H. (1991). *Episodic increases in stream acidity, catchment flow pathways and hydrograph separation*. PhD thesis, University of Cambridge.

Blake, G. (1965). Bulk density. *Methods of Soil Analysis. Part 1. Physical and Mineralogical Properties, Including Statistics of Measurement and Sampling*, (methodsofsoilana):374–390.

Boelter, D. H. (1965). Hydraulic conductivity of peats. *Soil Science*, 100(4):227–231.

Bogdon, C. (2013). Groundwater modeling numerical methods: Which one should you use? *Groundwater Modeling*.

Bouwer, H. and Rice, R. (1976). A slug test for determining hydraulic conductivity of unconfined aquifers with completely or partially penetrating wells. *Water resources research*, 12(3):423–428.

Branham, J. E. and Strack, M. (2014). Saturated hydraulic conductivity in sphagnum-dominated peatlands: do microforms matter? *Hydrological Processes*, 28(14):4352–4362.

Brümmer, C., Black, T. A., Jassal, R. S., Grant, N. J., Spittlehouse, D. L., Chen, B., Nesic, Z., Amiro, B. D., Arain, M. A., Barr, A. G., et al. (2012). How climate and vegetation type influence evapotranspiration and water use efficiency in canadian forest, peatland and grassland ecosystems. *Agricultural and Forest Meteorology*, 153:14–30.

Butler Jr, J. J. (1997). *The design, performance, and analysis of slug tests*. CRC Press.

Clymo, R. (2004). Hydraulic conductivity of peat at ellergower moss, scotland. *Hydrological Processes*, 18(2):261–274.

EEVblog Electronics Community Forum (2013). Batch Thermal Images Converter. $url : http : //www.eevblog.com/forum/thermal - imaging/flir - e4 - thermal - imaging - camera - teardown/msg350556/?PHPSESSID = b0284cea599a8c7c473ae23fff104b37$.

Eijkelkamp (2012). 08.60 Pycnometer gebruiksaanwijzing. url:https://www.eijkelkamp.com/download.php?file=a5562098.

Eppinga, M. B., De Ruiter, P. C., Wassen, M. J., and Rietkerk, M. (2009a). Nutrients and hydrology indicate the driving mechanisms of peatland surface patterning. *The American Naturalist*, 173(6):803–818.

Eppinga, M. B., Rietkerk, M., Wassen, M. J., and De Ruiter, P. C. (2009b). Linking habitat modification to catastrophic shifts and vegetation patterns in bogs. *Plant Ecology*, 200(1):53–68.

Ferrati, R., Canziani, G. A., and Moreno, D. R. (2005). Esteros del ibera: hydrometeorological and hydrological characterization. *Ecological modelling*, 186(1):3–15.

Foster, D., King, G., Glaser, P., and Wright, H. (1983). Origin of string patterns in boreal peatlands.

Franke, O. L., Reilly, T. E., and Bennett, G. D. (1987). *Definition of boundary and initial conditions in the analysis of saturated ground-water flow systems: an introduction*. US Government Printing Office.

Geuzaine, C. and Remacle, J.-F. (2009). Gmsh: A 3-d finite element mesh generator with built-in pre-and post-processing facilities. *International Journal for Numerical Methods in Engineering*, 79(11):1309–1331.

Gong, J., Wang, K., Kellomäki, S., Zhang, C., Martikainen, P. J., and Shurpali, N. (2012). Modeling water table changes in boreal peatlands of finland under changing climate conditions. *Ecological modelling*, 244:65–78.

Gorham, E. (1991). Northern peatlands: role in the carbon cycle and probable responses to climatic warming. *Ecological applications*, 1(2):182–195.

Greswell, R., Ellis, P., Cuthbert, M., White, R., and Durand, V. (2009). The design and application of an inexpensive pressure monitoring system for shallow water level measurement, tensiometry and piezometry. *Journal of hydrology*, 373(3):416–425.

Gupta, H. V., Kling, H., Yilmaz, K. K., and Martinez, G. F. (2009). Decomposition of the mean squared error and nse performance criteria: Implications for improving hydrological modelling. *Journal of Hydrology*, 377(1):80–91.

Haitjema, H. M. and Mitchell-Bruker, S. (2005). Are water tables a subdued replica of the topography? *Groundwater*, 43(6):781–786.

Hansen, K. (1959). The terms gyttja and dy. *Hydrobiologia*, 13(4):309–315.

Heijmans, M. M. P. D., Mauquoy, D., van Geel, B., and Berendse, F. (2008). Long-term effects of climate change on vegetation and carbon dynamics in peat bogs. *Journal of Vegetation Science*, 19(3):307–320.

Holden, J. and Burt, T. (2003). Hydraulic conductivity in upland blanket peat: measurement and variability. *Hydrological Processes*, 17(6):1227–1237.

Hvorslev, M. J. (1951). Time lag and soil permeability in ground-water observations.

Ise, T., Dunn, A. L., Wofsy, S. C., and Moorcroft, P. R. (2008). High sensitivity of peat decomposition to climate change through water-table feedback. *Nature Geoscience*, 1(11):763–766.

Ivanov, K. E. et al. (1981). *Water movement in mirelands.* Academic Press Inc.(London) Ltd.

Jackson, R., Reginato, R., and Idso, S. (1977). Wheat canopy temperature: a practical tool for evaluating water requirements. *Water Resources Research*, 13(3):651–656.

Jones, J. E. (1977). Calculation of evapotranspiration using color-infrared photography. *NASA STI/Recon Technical Report N*, 78:22345.

Joosten, H. and Clarke, D. (2002). Wise use of mires and peatlands.

Kalma, J. and Jupp, D. (1990). Estimating evaporation from pasture using infrared thermometry: evaluation of a one-layer resistance model. *Agricultural and Forest Meteorology*, 51(3-4):223–246.

Kaplan, D. A., Paudel, R., Cohen, M. J., and Jawitz, J. W. (2012). Orientation matters: Patch anisotropy controls discharge competence and hydroperiod in a patterned peatland. *Geophysical Research Letters*, 39(17).

Laiho, R. (2006). Decomposition in peatlands: Reconciling seemingly contrasting results on the impacts of lowered water levels. *Soil Biology and Biochemistry*, 38(8):2011–2024.

Limpens, J., Holmgren, M., Jacobs, C. M., Van der Zee, S. E., Karofeld, E., and Berendse, F. (2014). How does tree density affect water loss of peatlands? a mesocosm experiment. *PloS one*, 9(3):e91748.

Loisel, J. and Yu, Z. (2013). Surface vegetation patterning controls carbon accumulation in peatlands. *Geophysical Research Letters*, 40(20):5508–5513.

Lund Research Ltd (2013). Dependent T-Test using SPSS Statistics. url:https://statistics.laerd.com/spss-tutorials/dependent-t-test-using-spss-statistics.php.

Maes, W. and Steppe, K. (2012). Estimating evapotranspiration and drought stress with ground-based thermal remote sensing in agriculture: a review. *Journal of Experimental Botany*, 63(13):4671–4712.

Magnusson, T. (1994). Studies of the soil atmosphere and related physical characteristics in peat forest soils. *Forest Ecology and Management*, 67(1-3):203–224.

Mezbahuddin, M., Grant, R., and Flanagan, L. (2016). Modeling hydrological controls on variations in peat water content, water table depth, and surface energy exchange of a boreal western canadian fen peatland. *Journal of Geophysical Research: Biogeosciences*.

Moffett, K. B. and Gorelick, S. M. (2012). A method to calculate heterogeneous evapotranspiration using submeter thermal infrared imagery coupled to a stomatal resistance submodel. *Water Resources Research*, 48(1).

Moore, T., Roulet, N., and Waddington, J. (1998). Uncertainty in predicting the effect of climatic change on the carbon cycling of canadian peatlands. *Climatic change*, 40(2):229–245.

Nijp, J. J. (2015). *Fine scale ecohydrological processes in northern peatlands and their relevance for the carbon cycle*. PhD thesis, Wageningen University.

Nijp, J. J., Limpens, J., Metselaar, K., Peichl, M., Nilsson, M. B., Zee, S. E., and Berendse, F. (2015). Rain events decrease boreal peatland net co2 uptake through reduced light availability. *Global change biology*, 21(6):2309–2320.

Nijp, J. J., Metselaar, K., Limpens, J., Teutschbein, C., Peichl, M., Nilsson, M. B., Berendse, F., and van der Zee, S. E. (2016). Including hydrological self-regulating processes in peatland models: Effects on peatmoss drought projections. *Science of The Total Environment*.

Nilsson, M., Sagerfors, J., Buffam, I., Laudon, H., Eriksson, T., Grelle, A., Klemedtsson, L., Weslien, P., and Lindroth, A. (2008). Contemporary carbon accumulation in a boreal oligotrophic minerogenic mire–a significant sink after accounting for all c-fluxes. *Global Change Biology*, 14(10):2317–2332.

Nungesser, M. K. (2003). Modelling microtopography in boreal peatlands: hummocks and hollows. *Ecological Modelling*, 165(2):175–207.

Nyberg, L. (1995). Water flow path interactions with soil hydraulic properties in till soil at gårdsjön, sweden. *Journal of Hydrology*, 170(1):255–275.

Päivänen, J. et al. (1973). *Hydraulic conductivity and water retention in peat soils.* Suomen metsätieteellinen seura.

Peichl, M., Öquist, M., Löfvenius, M. O., Ilstedt, U., Sagerfors, J., Grelle, A., Lindroth, A., and Nilsson, M. B. (2014). A 12-year record reveals pre-growing season temperature and water table level threshold effects on the net carbon dioxide exchange in a boreal fen. *Environmental Research Letters*, 9(5):055006.

Price, J. S. (2003). Role and character of seasonal peat soil deformation on the hydrology of undisturbed and cutover peatlands. *Water Resources Research*, 39(9).

Ridolfi, L., D'Odorico, P., and Laio, F. (2006). Effect of vegetation–water table feedbacks on the stability and resilience of plant ecosystems. *Water Resources Research*, 42(1).

Rietkerk, M., Dekker, S. C., de Ruiter, P. C., and van de Koppel, J. (2004). Self-organized patchiness and catastrophic shifts in ecosystems. *Science*, 305(5692):1926–1929.

Rodhe, A. (1989). On the generation of stream runoff in till soils. *Hydrology Research*, 20(1):1–8.

Rubin, D. B. (1973). Matching to remove bias in observational studies. *Biometrics*, pages 159–183.

Rydin, H., Gunnarsson, U., and Sundberg, S. (2006). The role of sphagnum in peatland development and persistence. In *Boreal peatland ecosystems*, pages 47–65. Springer.

Rydin, H., Jeglum, J. K., and Jeglum, J. K. (2013). *The biology of peatlands, 2e*. Oxford university press.

Schlotzhauer, S. M. and Price, J. S. (1999). Soil water flow dynamics in a managed cutover peat field, quebec: Field and laboratory investigations. *Water Resources Research*, 35(12):3675–3683.

Seguin, B., Baelz, S., Monget, J.-M., and Petit, V. (1982). Utilisation de la thermographie ir pour l'estimation de l'évaporation régionale. i. mise au point méthodologique sur le site de la crau.

Silvola, J., Alm, J., Ahlholm, U., Nykanen, H., and Martikainen, P. J. (1996). Co_2 fluxes from peat in boreal mires under varying temperature and moisture conditions. *Journal of Ecology*, pages 219–228.

Strack, M. and Waddington, J. (2007). Response of peatland carbon dioxide and methane fluxes to a water table drawdown experiment. *Global Biogeochemical Cycles*, 21(1).

Swanson, D. K. and Grigal, D. F. (1988). A simulation model of mire patterning. *Oikos*, pages 309–314.

Tarnocai, C. (2006). The effect of climate change on carbon in canadian peatlands. *Global and planetary Change*, 53(4):222–232.

van der Schaaf, S. (1999). *Analysis of the hydrology of raised bogs in the Irish Midlands: a case study of Raheenmore Bog and Clara Bog*. Schaaf.

van Dijk, G., Nijp, J. J., Metselaar, K., Lamers, L. P., and Smolders, A. J. (2016). Salinity-induced increase of the hydraulic conductivity in the hyporheic zone of coastal wetlands. *Hydrological Processes*.

Vasander, H. and Kettunen, A. (2006). Carbon in boreal peatlands. In *Boreal peatland ecosystems*, pages 165–194. Springer.

Verry, E. (1997). Hydrological processes of natural, northern forested wetlands. *Northern forested wetlands: Ecology and management*, pages 163–188.

Westrene, E. v. (2017). *The relation between hydraulic conductivity, vegetation and peat soil characteristics of boreal peatlands*. PhD thesis, Wageningen University.

Whittington, P. N. and Price, J. S. (2006). The effects of water table draw-down (as a surrogate for climate change) on the hydrology of a fen peatland, canada. *Hydrological Processes*, 20(17):3589–3600.

Wieder, R. K. and Vitt, D. H. (2006). *Boreal peatland ecosystems*, volume 188. Springer Science & Business Media.

Wieder, R. K., Vitt, D. H., and Benscoter, B. W. (2006). Peatlands and the boreal forest. In *Boreal peatland ecosystems*, pages 1–8. Springer.

Wiedermann, M. M., Gunnarsson, U., Ericson, L., and Nordin, A. (2009a). Ecophysiological adjustment of two sphagnum species in response to anthropogenic nitrogen deposition. *New Phytologist*, 181(1):208–217.

Wiedermann, M. M., Gunnarsson, U., Nilsson, M. B., Nordin, A., and Ericson, L. (2009b). Can small-scale experiments predict ecosystem responses? an example from peatlands. *Oikos*, 118(3):449–456.

Yazaki, T., Urano, S.-i., and Yabe, K. (2006). Water balance and water movement in unsaturated zones of sphagnum hummocks in fuhrengawa mire, hokkaido, japan. *Journal of hydrology*, 319(1):312–327.

Yuan, J., Cohen, M. J., Kaplan, D. A., Acharya, S., Larsen, L. G., and Nungesser, M. K. (2015). Linking metrics of landscape pattern to hydrological process in a lotic wetland. *Landscape Ecology*, 30(10):1893–1912.

Zlotnik, V. A., Goss, D., and Duffield, G. M. (2010). General steady-state shape factor for a partially penetrating well. *Ground water*, 48(1):111–116.

Appendices

Appendix A - Catchment model

Prior to the model run with various pattern scenarios, it was the intent to create a model for the entire catchment, which would provide the initial conditions and boundary conditions for a smaller domain in which the patterns would be implemented. The aim was to have more realistic conditions for the smaller domain, as now only estimations are used; the initial condition is set fixed at a certain depth below the surface, whereas the catchment model could have shown variation within the smaller domain. The boundary conditions now have a fixed gradient along the slope, where the initial plan was to have a fixed flux, derived from the catchment model. However, the catchment model could not be used due to various complications in combination with time constraints. The decision was made to estimate the initial conditions and boundary conditions and only run the various pattern scenarios. In this appendix the methods used for the catchment model are described, and the complications discussed.

Many of the aspects of the smaller model were also used in the catchment model. As the aspects are described in detail in the methods, they are only mentioned and not thoroughly explained in this section.

Landscape elements

The domain of the model covered the entire Degerö Stormyr catchment and therefore contained other areas than only peat. These areas were either open water (small pools) or mineral outcrops. The mineral outcrops had higher elevation and consisted out of till covered with a shallow layer of weathered till, where at most locations pine trees were growing. Since the domain is larger than the one used for the pattern scenarios no hummocks or hollows were implemented. This resulted in a less dense needed node discretisation and thus a shorter model run time. The map with the used landscape elements was obtained in the same manner as the pattern maps; through classification in ArcMap. The open water entities were rejected from this map, as they covered a very small area and thus having little effect on the model run, whilst implementing them might lead to complications. At first the borders between the entities were sharp; there was no smooth transition between them. This led to high differences in hydraulic conductivity over a small spatial distance, which again led to instabilities in the model. As the differences were high, no correct state could be found, so the model kept iterating. When the source of this became known, a buffer around the entities was implemented. The selected distance was 35 meter, as this would ensure that at least one node was present in this area when looking at the spatial discretisation. The buffer contained a smooth transition from one entity to the other.

Boundary conditions, run time and discretisation

The boundary conditions were all set to no-flux except for the catchment outlet; a small stream. There the boundary condition was set to a fixed state of 1 meter below the peat surface, as was observed in the field. No validation or parameter estimation for this was done, as it was decided to skip this model before reaching that stage. One run was performed with a fixed state of 0.3 meter below the peat surface, bu this resulted in large errors near the outlet. The run time of the model lasted over one growing season (15-05 till 15-10). This was done to provide ample time for the model results not to be influenced by the initial conditions at the time of the scenario runs. The time period selected was the year 2006, as the smaller model would also run during this period. The small model run would start with the initial and boundary conditions from the catchment model at that time. The remainder of the time from the catchment model was planned to be used for the boundary conditions, as a peak in the groundwater is expected to flow through the smaller domain after the precipitation event. The temporal discretisation was set at daily time steps, as meteorological data was already present at this interval and this interval provides some detail while not resulting in very long run times. The method for the spatial discretisation for the nodes was the same as for the pattern model. A higher density was placed around areas of interest; the border of landscape elements and the domain used for the pattern model.

Geology and hydraulic conductivity

As described in section 2.1 the geology consists out of till with a peat layer on top. The hydraulic conductivity of the peat is implemented in the same manner as in the scenario model except that it is averaged for hummocks and hollows. Unlike the scenario model, the catchment model did include the till layer underneath the peat as it was expected to influence the hydrology when looking at catchment scale. The till depth was implemented through a depth to bedrock map, which showed the depth from the surface until the stone underneath the till layer. At the mineral outcrops, the till was covered by a shallow soil. This soil was assumed not be be present underneath the peat. Under the peat a gyttja layer is presumably present (gyttja is a mixture of organic material with other sediments (Hansen, 1959)). This was not taken into the account in the model.

The hydraulic conductivity was set as a function of both location and depth. The location showed whether it was on a mineral outcrop or peat, which determined the hydraulic conductivity values over depth. As no measurements were performed on the hydraulic conductivity of these outcrops in the field, the conductivity function was obtained from the paper by Bishop (1991) who performed a study on an area nearby. The peat and till both show a rapid decrease in conductivity as an exponential function (Amvrosiadi et al., 2016; Rodhe, 1989). The conductivity of the weathered layer was obtained by a study by Nyberg (1995) a bit more to the south of Sweden with the same vegetation type.

Porosity

The porosity in the catchment model is slightly more complicated as it varies over the landscape elements and over depth. If the groundwater level drops below the peat, the porosity value of till is used as $p = 0.55 * e^{(0.55*-GWL)}$. In the peat itself the same function is used as in the scenario model. At the reached stage of modelling the function was not smoothed yet. It was found that smoothing functions, to make sure no sudden differences appear, result in less unstable model runs, with less iterations needed.

Hydraulic conductivity

The hydraulic conductivity was implemented in the same manner as for the scenario model, but due to the more complex geology and the needed smoothing of the function, it became more complicated. A function for each entity (peat, weathered till and till) was created. All functions had the same exponential form which was obtained through data analysis (peat) or literature (till). As the hydraulic conductivity needed to be integrated over depth and more entities were on top of each other, the integral of each entity (over the entire depth for deeper layers, or from the groundwater level until the next entity) was summed. To make sure no spatially large differences in hydraulic conductivity occurred, and to make sure to represent the reality, the function was smoothed. On top of a mineral outcrop there was only till with a weathered layer on top. In the middle of the mire, there is only peat with a till layer underneath it. On the buffers between the outcrop and the peat a fading out zone of the weathered layer is implemented. At the mineral outcrop side the weathered depth is $1 * D_{weathered}$ and at the peat side it is $0 * D_{weathered}$. In between is a linear function that shows how the weathered layer is less formed underneath the peat. By doing so, no large variations in hydraulic conductivity occur at a small spatial scale. One thing that was not solved, is the smoothing over depth. No large differences are expected as the integral is taken over the entire depth, but this was not tested yet.

Evapotranspiration

The evapotranspiration was first implemented directly from the meteorological data. The data had a daily interval, same as the model run. No spatial variation was implemented yet. The model did not perform well on this and kept iterating. Then evapotranspiration was implemented as a function of the groundwater level (the same as the scenario model). No variation between hummock and hollow was used, but variation between peat and forest, as the mineral outcrops contained pine trees. In the model this led to instability. The cause for this was not yet found.

Complications

The built up of this model was through trial and error, many errors were encountered of which a lot were solved. At the current stage of the model, no errors or instabilities are present, though they might appear when running the model for the entire runtime (only a few time steps were tested due to the long runtime). The model was not validated yet, so it is not known whether the model is a good representation of the catchment and can therefore be used for the initial state and boundary condition of the scenario model. Though no direct errors were found, it was decided not to work further on this model. At the stage it was left, the predicted run time was at least 2 months, due to multiple needed iterations and many nodes on which the equations had be performed on. By smoothing various functions as explained above, the run time was already improved. As this study had some time constraints it was decided that further improving on the catchment model would take too much time, that was needed for the scenario models.

For further studies this model could be improved by further smoothing every function (e.g. the porosity over depth) or write the code more efficiently so the model will perform faster. Another option is to built a model in a different environment (e.g. Modflow). This may lead to different complications, but the environment it is built in now, was not created for such big models, but rather as a simple example during lectures.

Appendix B - Geological map

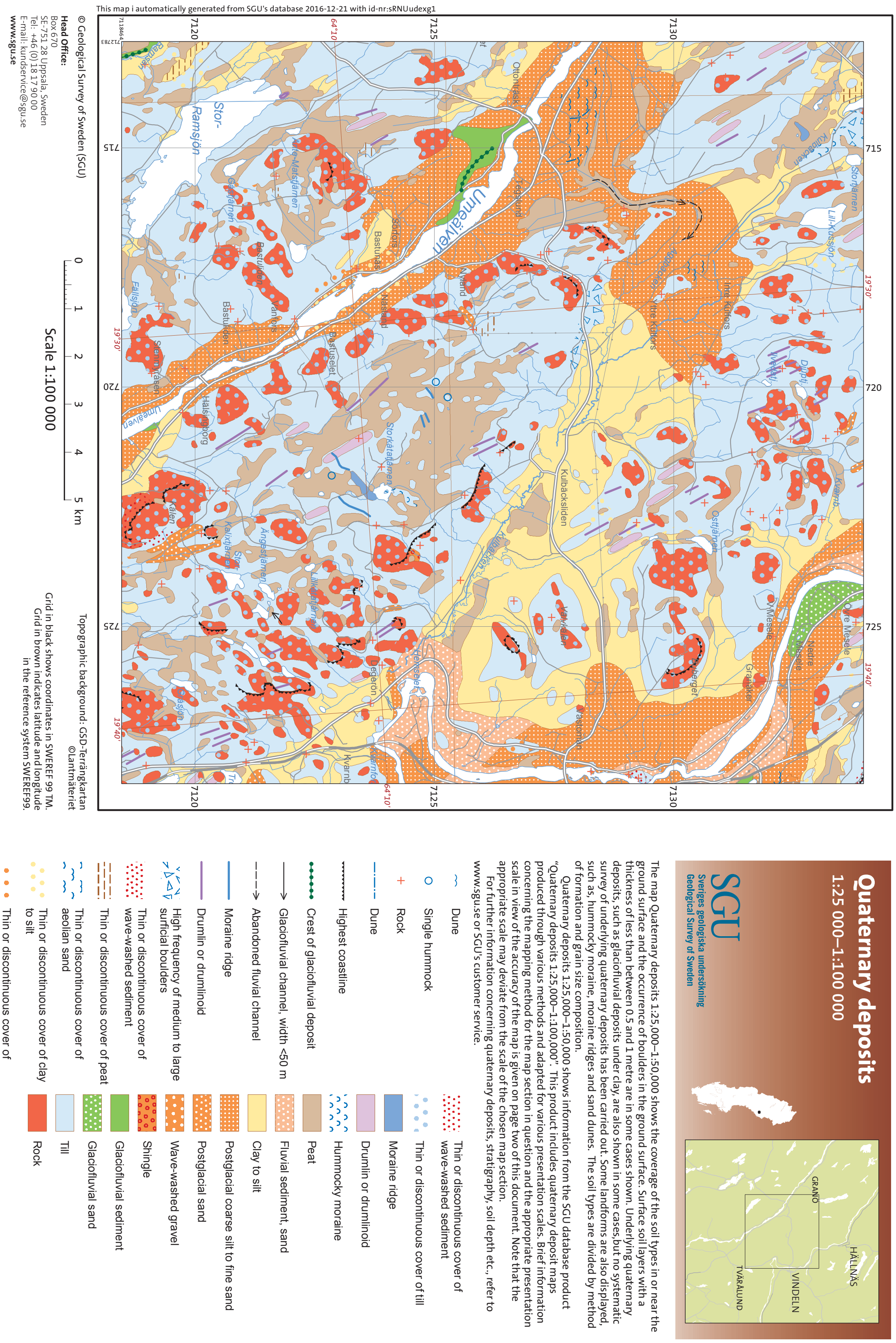

Appendix C - Metadata field measurements

In the period from 20-06-2016 till 20-07-2016, 138 hydraulic conductivity measurements were performed. Only 87 of these measurements could be used for the calculation of the hydraulic conductivity. The remaining measurements showed either too much noise, were constant after water addition or a problem with the diver itself arose; some divers broke down or the wrong time interval was set, leaving too little data points on the peak to calculate the hydraulic conductivity. Of the 87 useful measurements 21 had an increase in pressure after water addition, so the second method was applied for calculation (section 2.3.2). Of the 87 hydraulic conductivity values, 41 are hummocks and 45 are hollows. There are 9 reference measurements in the reference hummock, and 6 in the reference hollow. The distribution of measurements over pattern size and over depth can be found in table 1.

Table 1: Top: the distribution of measurements over hummock and hollow size (the reference measurements are here averaged and seen as 1 measurement to prevent over representation, leading to a total of 73 measurements). Bottom: the distribution of measurements over depth for hummocks and hollows.

Pattern entity	Small	Large	Total
Hummock	16	19	35
Hollow	21	17	38

Hummock depths [cm]	n	Hollow depths [cm]	n
10-20	11	10-20	12
30-40	9	30-40	12
60-70	6	60-70	9
100-110	8	100-110	3
150-160	1	150-160	2

In total 134 infra red pictures were taken over 8 different days in order to study evapotranspiration differences between hummocks and hollows. Of these photos 71 were taken from hollows, 63 from hummocks. The weather conditions varied over the days and often during one day. Therefore the photos were taken under various weather conditions; cloudless, slight cloud cover, cloudy and slight rain. The weather conditions were kept as similar as possible during one measurement day, for example by waiting till a cloud passed to measure under sunny conditions.

Appendix D - Porosity prediction

In the figures below, the observed porosity values are compare with the predicted values.

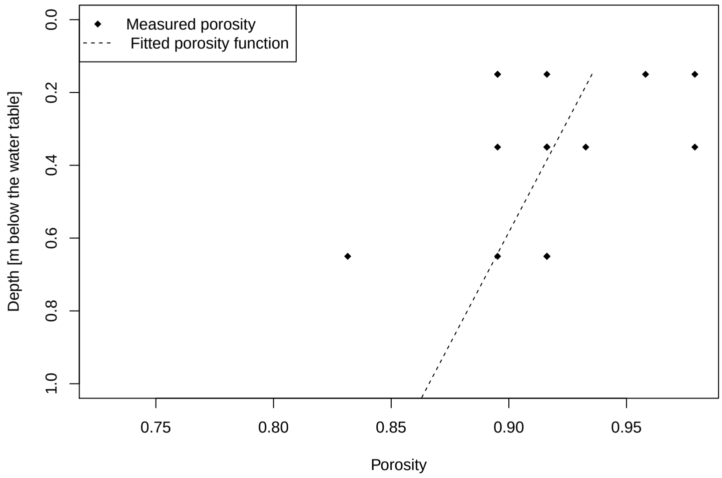

Figure 1: The measured porosity values over depth, with the fitted function (dotted line)

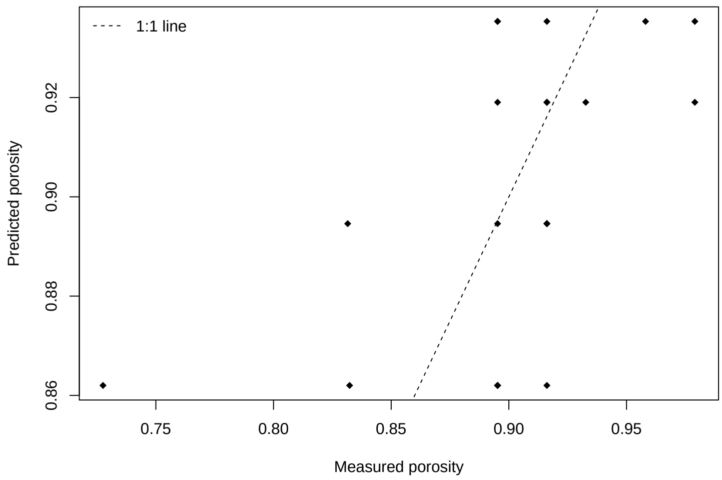

Figure 2: The relation between the observed and predicted porosity values. The RMSE is 0.04, and R^2 is 0.295